

Random Spiking and Systematic Evaluation of Defenses Against Adversarial Examples

Huangyi Ge* Sze Yiu Chau* Ninghui Li*

{geh, schau, ninghui}@purdue.edu, Purdue University, West Lafayette, Indiana, USA*

Abstract—Image classifiers often suffer from adversarial examples, which are generated by adding a small amount of noises to input images to trick classifiers into misclassification. Over the years, many defense mechanisms have been proposed, and different researchers have made seemingly contradictory claims on their effectiveness. We argue that such discrepancies are primarily due to inconsistent assumptions on the attacker’s knowledge. To this end, we present an analysis of possible adversarial models, and propose an evaluation framework for comparing different defense mechanisms. As part of the framework, we introduced a more powerful and realistic adversary strategy. We propose a new defense mechanism called Random Spiking (RS), which generalizes dropout and introduces random noises in the training process in a controlled manner. With a carefully chosen placement, RS incurs negligible negative impact on prediction accuracy. Evaluations under our proposed framework suggest RS delivers better protection against adversarial examples than many existing schemes.

I. INTRODUCTION

Modern society is increasingly reliant upon software systems trained by machine learning techniques. Many such techniques, however, were designed under the implicit assumption that both the training and test data follow the same static (although possibly unknown) distribution. In the presence of intelligent and resourceful adversaries, this assumption may no longer hold. A malicious adversary can deliberately manipulate an input instance to make it deviate from the distribution of the training/testing dataset, and cause the learning algorithms and the trained models to behave unexpectedly. For example, it is found that existing image classifiers based on Deep Neural Networks are highly vulnerable to adversarial examples [1], [2]. Often times, by modifying an image in a way that is barely noticeable by humans, the classifier will confidently classify it as something else. This phenomenon also exists for classifiers that do not use neural networks, and has been called “optical illusions for machines”.

Many approaches have since been proposed to help defend against adversarial examples. For example, Goodfellow et al. [1] proposed adversarial training, in which one trains a neural network using both the original training dataset and the newly generated adversarial examples. In region-based classification [3], one changes the process of inference. When given an input instance, one generates multiple instances by adding small amount of randomly generated noises to the original instance, collects the predictions on all perturbed instances, and uses majority voting to make the final prediction. Some approaches attempt to train additional neural network models to identify and reject adversarial examples [4], [5].

Understanding why adversarial examples work and how to defend against them are becoming increasingly important, as machine learning techniques are used ubiquitously, for example, in transformative technologies such as autonomous cars, unmanned aerial vehicle, and so on.

While the research community has seen a proliferation in proposals of defense mechanisms, we argue that a satisfactory evaluation and a fair head-to-head comparison of different mechanisms is still missing. On one side of the spectrum, papers proposing defense mechanisms often conduct a simplistic evaluation of their proposal assuming the attacker has no knowledge of the defense itself, demonstrating close to 100% effectiveness. Such evaluations fail to consider stronger yet meaningful adversarial models. On the other end of the spectrum, some papers demonstrate that existing proposed defenses can still be overcome use a very strong adversarial model assuming that all parameters are known, or does not provide measurements of whether overcoming the defense requires a significant increase in its distortion. This approach fails to recognize progress made in the right direction, even if a defense is not 100% effective.

Such inconsistencies in evaluation methodology leads to seemingly contradictory claims regarding model robustness, and hinders the progress of the field. In Section III, we present a careful analysis of possible adversarial models, and propose to focus on what we call translucent-box attacks, in which the adversary is assumed to know the defense mechanism, model architecture, training dataset, training methods, but not the precise parameters of the target model. With this knowledge, the adversary can use the same training process that is used to generate the target model to train one or more **shadow models**, and to generate adversarial examples leveraging such shadow models. Such adversarial examples are grouped based on their degree of perturbation. (We use L_2 norm in this paper, but other metrics can be used as well.) We then evaluate the percentage of adversarial examples that successfully fool the target model, i.e., the **transferability rate**.

This model is reminiscent of the Kerckhoffs’s principle embraced by cryptographers, which states the security of a cryptosystem depends only on the secrecy of the key (and the randomness used in generating it) but not any knowledge about the system itself.

While generating adversarial examples based on shadow models and then assessing transferability is nothing new. Existing application of this method does not fully exploit the potential of shadow models, and will overestimate the

effectiveness of any defense. We propose two improvements. First, one can train many shadow models under the same configuration (with different randomness), and then generate adversarial examples that can simultaneously fool multiple shadow models at the same time. Second, one can reserve some shadow models as “validation models”. These validation models are not used when generating adversarial examples; however, generated adversarial examples are first run against them, and only those examples that are able to fool certain percentage of the validation models are used in evaluation against the target model. This models a more determined and resourceful attacker who is willing to spend more resources to find more effective adversarial examples to deploy, a scenario that is certainly realistic. Our experimental results demonstrate that these more sophisticated adversary strategies lead to significantly higher transferability rates.

Furthermore, in Section IV, we propose a new defense mechanism called Random Spiking, where random noises is added to one or more hidden layers during training. Random Spiking generalizes the idea of dropout [6], where hidden units are randomly dropped during training. In Random Spiking, the outputs of some randomly chosen units are set to a random noise. The intuition is that models trained with Random Spiking generalizes better and should be able to better handle adversarial examples, which can be viewed as injecting (albeit non-random) noises in the input.

In Section V, we present extensive evaluations of several existing defense mechanisms and Random Spiking (RS) using our proposed framework, and empirically show that RS, especially when combined with adversarial training, tends to make the models more resilient to adversarial examples.

In summary, we make three contributions. (1) The proposed evaluation methodology, especially the more powerful and realistic adversary strategy of attacking multiple shadows in parallel and using validation models to filter. (2) The idea of Random Spiking, which is demonstrated to offer additional resistance to adversarial examples. We conjecture that, like Dropout, Random Spiking might be able to improve generalization in some contexts. (3) We provide a thorough evaluation of several defense mechanisms against adversarial examples, improving our understanding of them.

II. BACKGROUND

A. Neural Network Models

We consider neural networks that are used as m -class classifiers, where the output of a network is computed using the softmax function. Given such a neural network used for classification, let $\mathbf{z}(x)$ denote the vector output of the final layer before the softmax activation, and $C(x)$ denote the classifier defined by the neural network. Then,

$$C(x) = \arg \max_i \left(\exp(\mathbf{z}(x)_i) / \left(\sum_{j=1}^n \exp(\mathbf{z}(x)_j) \right) \right).$$

Oftentimes, $\exp(\mathbf{z}(x)_i) / \left(\sum_{j=1}^n \exp(\mathbf{z}(x)_j) \right)$ is interpreted as the probability that the input x belongs to the i -th category, and the classifier chooses the class with the highest probability.

Under this interpretation, the output $\mathbf{z}(x)$ is related to log of probabilities, and we thus call $\mathbf{z}(x)$ the **logits output**.

B. Adversarial Examples

Given a dataset D of instances, each of the form (x, y) , where x gives the features of the instance, and y the label of the instance, and a classifier $C(\cdot)$ trained using a subset of D , we say that an instance x' is an *adversarial example* if and only if **there exists an instance $(x, y) \in D$ such that x' is close to x , $C(x) = y$, and $C(x') \neq y$.**

Note that in the above we did not define what “ x' is close to x ” means. Intuitively, when x represents an image, by closeness we mean human perceptual similarity. However, we are unaware of any mathematical distance metric that accurately measures human perceptual similarity. In the literature L_p norms are often used as the distance metric for closeness. L_p is defined as

$$L_p(x, x') = \|x - x'\|_p = \left(\sum_{i=1}^n |x_i - x'_i|^p \right)^{1/p}.$$

The commonly used L_p metrics include: L_0 , the number of changed pixels [7]; L_1 , the sum of absolute values of the changes in all pixels [8]; L_2 , the Euclidean norm [9], [10], [1], [11]; and L_∞ , the maximum absolute change of any pixels [2]. In this paper, we use L_2 , which reflects both the number of changed pixels and the magnitude of their change. We call $L_2(x, x')$ the **distortion** of the adversarial example x' .

When generating an adversary example against a classifier $C(\cdot)$, one typically starts from an existing instance (x, y) and generates x' . In an **untargeted attack**, one generates x' such that $C(x') \neq y$. In a **targeted attack**, one has a desired target label $t \neq y$ and generates x' such that $C(x') = t$.

Goodfellow *et al.* [2] proposed the fast gradient sign (FGS), which generates the adversarial example based on the gradient sign of the loss value according to the input image. To our knowledge, currently the most effective attack is the one proposed by Carlini and Wagner [9], which we call the **Iterative Optimization** attack. In a targeted attack, given a neural network with logits output \mathbf{z} , an input x , and a target class label t , the attack tries to solve the following optimization problem:

$$\arg \min_{x'} (\|x - x'\|_p + c \cdot l(x')) \quad (1)$$

where the loss function l is defined as

$$l(x') = \max(\max\{\mathbf{z}(x')_i : i \neq t\} - \mathbf{z}(x')_t, -K).$$

Here, K is called the **confidence value**, and is a positive number that one can choose. Intuitively, we desire $\mathbf{z}(x')_t$ to be higher than any $\mathbf{z}(x')_i$ where $i \neq t$ so that the neural network predicts label t on input x . Furthermore, we prefer the gap in the logit of the class t and the highest of any class other than t to be as large as possible (until the gap is K , at which point we consider the gap to be sufficiently large). With a larger K , the optimization finds adversarial instances that are classified to t with a higher confidence. In general, choosing a large value K would result in adversarial examples that may

have a higher distortion, but will be classified to the desired label with higher confidence. The parameter $c > 0$ in Eq. 1 is a regularization constant to adjust the relative importance of minimizing the distortion versus minimizing the loss function l . In the attack, c is initially set to a small initial value, and then dynamically adjusted based on the progress made by the iterative optimization process.

The Iterative Optimization attack uses the Adam algorithm [12] to solve the optimization problem in Eq. 1. Adam performs iterative gradient-based optimization, based on adaptive estimates of lower-order moments. Compared to other attacks, such as FGS, the Iterative Optimization attack is more time-consuming. However, it is able to find more effective adversarial examples.

C. Existing Defenses

Many approaches have been proposed to help defend against adversarial example. Here we give an overview of some of them.

1) *Adversarial Training*: Goodfellow *et al.* [2] proposed adversarial training, which trains a neural network using both the training dataset and newly generated adversarial examples. In [2], it is shown that models that have gone through adversarial training provide some resistance against adversarial examples generated by the FGS method. Performing adversarial training requires generating adversarial examples. Since the Iterative Optimization attack takes a long time to generate adversarial examples, conducting adversarial training significantly increases the training time.

2) *Defensive Distillation*: Distillation training was originally proposed by Hinton *et al.* [13] for the purpose of distilling knowledge out of a complicated model to train a model that has a smaller size. Given a model whose knowledge one wants to distill, one applies the model to each instance in the training dataset and generates a probability vector, which is used as the new label for the instance. This is called the soft label, because, instead of a single class, the label includes probabilities for different classes. A new model is trained using training instances with soft labels. The intuition is that the probabilities, even those that are not the largest in a vector, encode valuable knowledge. To make this knowledge more pronounced, the probability vector is generated after dividing the logits output with a temperature constant $T > 1$. This has the effect of making the smaller probabilities larger and more pronounced. The new model is trained with the same temperature. However, when deploying the model for prediction, temperature is set to 1.

Defensive Distillation [14] is motivated by the original distillation training proposed by Hinton *et al.* [13]. The main difference between the two training methods is that defensive distillation uses the same network architecture for both initial network and distilled network. This is because the goal of using Distillation here is not to train a model that has a smaller size, but to train a more robust model.

3) *Region-based Classification*: Cao and Gong [3] proposed region-based classification to defend against adversarial

examples. Given an input, region-based classification first generates $m > 1$ perturbed inputs by adding bounded random noises to the original input, then computes a prediction for each perturbed input, and finally use voting to make the final prediction. This method slows down prediction by a factor of m . Evaluation in [3] shows that this can withstand adversarial examples generated by the Iterative Optimization attack under low confidence value K . However, if one increases slightly the confidence value K when generating the adversarial examples, this defense is no longer effective.

4) *MagNet*: Meng and Chen [4] proposed an approach that is called MagNet. MagNet combines two ideas to defend against adversarial examples. First, one trains detectors that attempt to detect and reject adversarial examples. Each detector uses an autoencoder, which is trained to minimize the L2 distance between input image and output. A threshold is then selected using validation dataset. The detector rejects any image such that the L2 distance between it and the encoded image is above the threshold. Multiple detectors can be used. Second, for each image that passes the detectors, a reformer (another autoencoder) is applied to the image, and the output (reformed image) is sent to the classifier for classification.

The evaluation of MagNet in [4] considers only adversarial examples generated without knowledge of the MagNet defence, on the ground that the Iterative Optimization attack requires knowledge of a target Neural Network, whereas MagNet has multiple Neural Networks involved. In [11], an effective attack is carried out against MagNet by adding to the optimization objective a term describing the goal to evade the detectors. Since one can combine all involved neural networks into a single one, one can apply the Iterative Optimization attack on the composite network.

III. TOWARDS A SYSTEMATIC EVALUATION METHODOLOGY

Previous proposals on defense mechanisms all contain experimental evaluations demonstrating their efficacy in defending against adversarial examples, often with close to 100% effectiveness. However, oftentimes subsequent research efforts show experimental results that appear to show that those defense proposals fail to provide adequate protection. Such apparent inconsistencies signify the lack of accepted methodology for evaluating and comparing the effectiveness of defense mechanisms. We discuss several factors that we believe have contributed to the different and sometimes mutually contradictory claims found in previous works, and propose a systematic evaluation methodology.

A. Adversary Knowledge

Adversary model plays an important role in any security evaluation. One important part of the adversary model is the assumption on adversary's knowledge. Below we first discuss the main categories of assumptions on the adversary's knowledge, and then discuss the alternatives.

- **Knowledge of Model (white-box)**. The adversary has full knowledge of the target model to be attacked, in-

cluding the model architecture, defense mechanism, and all the parameters, including those used in the defense mechanisms. We call such an attack a **white-box** attack.

- **Complete Knowledge of Process (translucent-box).** The adversary does not know the exact parameters of the target model. However, the adversary has complete knowledge of the training process, including the training datasets, model architecture, defense mechanism, and training algorithm. With this knowledge, the adversary can use the same training process that is used to generate the target model to train one or more **shadow models**. Depending on the degree of randomness involved in the training process, the shadow models may be very similar or quite different from the target model, and adversarial examples generated by attacking the shadow model(s) may or may not work very well. The property of whether an adversarial example generated by attacking one or more shadow models can also work against another target model is known as **transferability**. We call such an attack a **translucent-box attack**.

Technically, it is possible for a white-box adversary to know less than a translucent-box adversary *in some aspects*. For example, a white-box adversary may not know the training dataset. However, for the purpose of generating adversarial examples, knowing all details of the target model (white-box) is strictly more powerful than knowing the training process (translucent-box).

- **Adaptive translucent-box.** In addition to the training process, the adversary also has oracle access to the target model. That is, the adversary can query the target model with instances and receive the output.

The exact impact of such adaptive adversary on adversarial examples is far from being understood. For one thing, it depends on how much information is returned by the oracle access. The target model may return only the chosen label with a coarse-grained confidence value for that class, or a high-precision confidence vector for all labels. As an example of the impact of oracle access, it has been shown that an adversary can query the target model to build a synthetic training dataset, which can then be used to generate adversarial examples when the adversary does not have access to the original training dataset [15]. This is however only the tip of the iceberg. It is conceivable that an adversary can learn a lot of information about the parameters of a model by querying it, blurring the distinction between white-box and translucent-box. Furthermore, an attacker may be able to generate an adversarial example, using that example to query the target model, and then adjust the adversarial example based on the results returned by the target model. This is reminiscent of the adaptive attack models used for cryptanalysis. More research is needed to understand the potential impact of oracle access. In this paper, we limit our focus to white-box and translucent-box adversaries and leave adaptive translucent-box for future work.

If a defense mechanism uses one model for classification and separate models for detection of adversarial examples or processing of instances, then one could potentially assume different adversary knowledge for each of those models. For example, in a recent attack against the MagNet defense [11], the attacker is assumed to have Knowledge of Model on the classification model, but only Knowledge of Process on the defensive models.

Remark on “black-box” attack. The term black-box is often used in the literature, and is often defined as the adversary has only oracle access to the target model. For several reasons, we feel that the term “Black-Box” is ill-defined. First, as discussed above, we do not yet understand what capability oracle accesses give the adversary, and it could be that fine-grained oracle access (those with high-precision confidence vectors in the output) to the target model leads to very precise estimation of model parameters, equating black-box with white-box. In fact, in most usage of black-box in the literature, the attacker does not take advantage of such oracle accesses. Thus they are really referring to some non-adaptive gray-box adversary. Second, an adversary will have some knowledge about the target model under attack, e.g., the neural network architecture and the training algorithm, since given a task, the number of commonly used architectures is small.

In most usage of “black-box attack” in the literature, the intended meaning is that the adversary either does not know, or does not take advantage of any knowledge of the defense mechanism. Thus the adversary carries out the attack as if there is no defense. Indeed, many papers, when proposing a new defense mechanism, evaluate the efficacy of the proposed mechanisms under such a model. That is, the evaluation is conducted using adversarial examples that are generated without taking the defense itself into consideration. We argue that such an evaluation has limited values in understanding the security benefits of a defense mechanism, as it is a clear deviation from the Kerckhoffs’s principle. Later when the seemingly effective defense mechanisms are evaluated under a stronger adversary model, the efficacy is shown to be not as good as originally claimed, resulting in the contradictory conclusions.

Different Shades of Gray. The translucent-box model can be viewed a light-gray box, and can be relaxed in several orthogonal dimensions, to model an adversary that has incomplete knowledge of the training process. For example, the adversary may not have exact knowledge of the training dataset, but know only the general distribution of it. Another relaxation is that the adversary is aware that some defense is deployed, but is unsure which particular defense mechanism has been deployed. Thus the adversary can choose to generate adversarial examples that can do well against multiple defense mechanisms.

Our Choice of Adversary Model. We argue that defense mechanisms should be evaluated under both white-box and translucent-box attacks. Effective defense against white-box attacks is the ultimate objective. However, it is not imme-

diately clear whether such a goal is achievable, given our limited understanding of how and why Neural Networks work. Until defense in the white-box model is achieved, effective defense against translucent-box attacks is valuable and help the research community make progress.

translucent-box is quite a realistic assumption especially in an academic setting, as published papers generally include descriptions of the architecture, training process, defense mechanisms and the exact dataset used in their experiments. Robustness and security evaluations under this assumption is also consistent with the Kerckhoffs’s principle. In the rest of this paper, for the evaluation of proposed defense mechanisms, we will focus on translucent-box attacks.

We also note that there are two possible flavors of attacks. Focusing on image classifiers, the goal of an *untargeted attack* is to generate adversarial examples such that the classifier would give any output labels different from what human perception would classify. A *targeted attack* would additionally require the working adversarial examples to induce the classifier into giving specific output labels of the attacker’s choosing. In this paper, we consider only targeted attacks when evaluating defense mechanisms, as it models an adversary with a more specific objective.

B. Parameter Choice and Data Interpretation

Training a defense mechanism often requires multiple parameters as inputs. For example, a defense mechanism may be tuned to be more vigilant against adversarial examples, at the cost of reduced classification accuracy. When comparing defense mechanisms, we propose to choose parameters in a way that the classification accuracy on test dataset is similar.

At the same time, when using the Iterative Optimization attack to generate adversarial examples, an important parameter is the confidence value K . A defense mechanism may be able to resist adversarial examples generated under a low K value, but may prove much less effective against those generated under a higher value K . Using the same K value for different defenses, however, may not be sufficient for providing a level playfield of comparison. The K value represents inputs into the algorithm, and what really matters are the quality of the adversarial examples. We propose to run the Iterative Optimization attack against a defense mechanism under multiple K values, and group the resulting adversarial examples based on their distortion. We can then compare how well a defense mechanism performs adversarial examples with similar amount of distortion.

C. Adversary Strategy

Even after the assumption about the adversary’s knowledge is made, there are still many possibilities regarding what strategy the adversary takes. For example, when evaluating a defense mechanism under the translucent-box assumption, a standard method is to train m models, and, for each model, generate n adversarial examples. Then for each of the m model, treat it as the target model, and feed the $(m - 1)n$

adversarial examples generated on other models to it, and report the percentage of success among the $m(m - 1)n$ trials.

Such an evaluation method is assessing the success probability of the following naive adversary strategy: The adversary trains one shadow model, generates an adversarial example that works against the shadow model, and then deploy that adversarial example. A real adversary, however, can use a more effective strategy. It can try to generate adversarial examples that can fool multiple shadow models at the same time. After generating them, it can first test whether the adversarial examples can fool shadow models that are not used in the generation.

For any defense mechanism that is more effective against adversarial examples under the translucent-box attack than under the white-box model, the additional effectiveness must be due to the randomness in the training process. When that is the case, the above adversary strategy would have much higher success rate than the naive adversary strategy. Evaluation should be done against this adversary strategy (or more powerful ones when they are developed in the future).

We thus propose the following procedure for evaluating a defense mechanism in a translucent-box attack. One first trains $t + v$ shadow models. Then a set of t models are randomly selected, and adversarial examples are generated that can *simultaneously* attack all t of them; that is, the optimization objective of the attack includes all t models. For each of the remaining v models, held it out as the target model, use the $v - 1$ model as validation models, and an adversarial example is selected only when it fool a certain fraction of the validation models. Only for the examples that pass the validation stage, do we record whether it successfully transfer to the target model or not. The percentage of the successful transfer is used for evaluation. We will also group these examples under the degree of distortion and compute average transferability rate for each group. In our experiments, we use $t = v = 8$, and an example is selected when it can successfully attack at least 5 out of 7 validation models.

IV. OUR PROPOSED DEFENSE METHOD

So far, existing defense mechanisms have shown limited effectiveness. In addition, these defenses mechanisms often incur significant overhead. For example, region-based classification, in which one classifies multiple perturbed instances and then use majority vote for classification, significantly slows down the classification process. Ideally a defense mechanism should offer protection against adversarial examples without incurring significant overhead either in training or in evaluation.

We propose a general defense mechanism for deep neural networks. Two key insights drive our proposal. First, the existence of adversarial examples is an effect of over-fitting the distribution of both training and testing instances. For any task, meaningful input instances such as those in training and testing datasets are only a tiny fraction of all possible instances. For example, the vast majority of possible images (such as any image generated by sampling each pixel from a uniform distribution) cannot occur in training or testing.

Overfitting this distribution cannot be detected by using testing instances, since they are also in this distribution. Adversarial examples go outside this distribution, and are thus classified incorrectly. Second, while effective defense against white-box attacks is most desirable, it appears that achieving that is very difficult with our current, limited understanding of how and why complicated classifiers such as Deep Neural Networks are effective. Whenever a classifier has a complex decision boundary, knowing the precise boundary would enable one to find instances that are close to a given instance and yet is classified differently. If effective defense against white-box attacks is infeasible, then our best hope is to increase the degree of randomness in the training process, so that adversarial examples generated on the shadow models do not transfer well.

In this section, we first present the overview of Dropout [6], a technique originally aimed at preventing neural network from over-fitting through the introduction of some level of random noise. Then, we present **Random Spiking (RS)**, a randomized technique inspired by Dropout.

A. Dropout

Dropout is a technique for addressing overfitting [6]. The term “dropout” refers to dropping out units, i.e., temporarily removing the units along with all its incoming and outgoing connections from a network. In the simplest case, during each training epoch, each unit is retained with a fixed probability p independent of other units, where p can be chosen using a validation set or can simply be set at 0.5, which was suggested by the authors of [6]. More commonly, Dropout is selected applied to some layers in a DNN. There are several intuitions why Dropout is effective. One is that after applying Dropout, one is always trained with a subset of the units in the NN. This prevents units from co-adapting too much. That is, a unit cannot depend on the existence of another unit, and needs to learn to do something useful on its own. Another intuition is that training with Dropout approximates simultaneous training of an exponential numbers of “thinned” networks. During the testing, without applying the Dropout, the prediction approximates the averaging output of all these thinned networks.

Since Dropout introduces randomness in the training process, two models that are training with Dropout are likely to be less similar than two models that are trained without using Dropout. We show that indeed dropout shows a small degree of effectiveness on defending against adversarial example. For example, adversarial generated on models trained with Dropout have higher L_2 distortion.

B. Random Spiking

Dropout can be interpreted as a way of regularizing a neural network by adding noise to its hidden units. The idea of adding noise to the states of units has also been used in the context of Denoising Autoencoders (DAEs) by Vincent et al. [16], [17] where noise is added to the input units of an autoencoder and the network is trained to reconstruct the noise-free input.

Dropout generalizes this idea by changing the behavior of both the input units and the hidden units. However, instead of adding random noises, in Dropout, values are set to zero.

Our proposed approach generalizes Dropout and Denoising Autoencoders. Instead of training with removed units or injecting random noises into the input units, we inject random activations into some hidden units during the training process. The intuition of this is two-fold. First, adversarial examples make only small perturbations on benign images that do not significantly affect human perception. These perturbations inject noises that will be amplified through multiple layers and change the prediction of the networks. Random Spiking trains the network to be more robust to such noises. Second, if one needs to increase the degree of randomness in the training process beyond Dropout, using random noises instead of setting activations to zero is a natural approach.

More specifically, one adds a filtering layer in between two layers of nodes in a DNN. The effect of the filtering layer may change the output values of units in the earlier layer, affecting the values going into the later layer. With probability p , a unit’s value is kept unchanged. With probability $1 - p$, a unit’s value is set to a randomly sampled noise. If a unit has its output value thus randomly perturbed, in back-propagation we do not propagate anything backward through this unit, since any gradient computed is related to the random noise, and not the actual behavior of this unit. For layers after the Random Spiking filtering layer, back-propagation update would occur normally.

Currently, we use the Random Spiking filtering layer just once. Our experiments suggest that adding the Random Spiking layer to the later part of a network negatively affects prediction accuracy, and the impact on accuracy when adding it to an earlier layer is small. There are two explanation for that. First, since units chosen to have random noises stop back-propagation, having them later in the network have more impact on training. Second, when random noises are injected early in the network, there are more layers after it, and there is sufficient capacity in the model to deal with such noises without too much accuracy cost. When random noises are injected late, fewer layers exist to deal with their effect, and the network lacks the capacity to do so.

C. Generating Random Noises

To implement Random Spiking, we have to decide how to sample the noises that are to be used to replace the unit outputs. Sampling from a distribution with a fixed range is problematic because the impact of a noise depends on the distribution of other values in the same layer. If a random noise is too small compared to other values in the same layer, then its randomization effect is too small. If, on the other hand, the magnitude of the noise is a lot larger than the other values, it overwhelms the network.

In our approach, we compute the minimum value and maximum value among all values in the layers to be filtered, and sample a uniform random a value in that range. Since training NN is often done using mini-batches, the minimum

and maximum values are computed from the whole batch. More specifically, for a mini-batch B (a group of instances), let $O(B)$ be the output of the layer on B before the Random Spiking layer. If a neuron output $u_{ij} \in O(B)$ is chosen to be replaced by noise, then we choose a noise value uniformly at random $u'_{ij} \in [\min(O(B)), \max(O(B))]$.

V. EXPERIMENTAL EVALUATION

In this section, we present our evaluations on the various defense mechanisms. We first describe the methods and parameters used in the training of models (Section V-A). Then we discuss the use of techniques such as *bagging*, Dropout and Random Spiking in *prediction* (Section V-B). Next, we evaluate proposed defense mechanisms with model stability (Section V-C). We then demonstrate the merits of using multiple shadow models in attacks (Section V-D), and present further evaluations using better attack strategies in the white-box (Section V-E) and translucent-box settings (Section V-F).

A. Dataset and Model Training

For all of our experiments, we consider the following three datasets: *MNIST* [18], which consists of 70,000 8-bit grayscale images of handwritten digits (0-9), each has a resolution of 28×28 pixels; *Fashion-MNIST* [19], which includes 70,000 8-bit grayscale images at the resolution of 28×28 pixels, divided equally into 10 classes of fashion products (e.g. T-Shirt, Dress, etc.); *CIFAR-10* [20], which contains 60,000 True color (24-bit color depth) images at the resolution of 32×32 pixels, divided equally into 10 object classes (e.g., truck, airplane, etc.). Each dataset comes with 10,000 images selected for testing, and the remaining ones are for training.

In our experiments, we consider 9 schemes equipped with different defense mechanisms, all of which share the the same network architectures and training parameters (see Table VII and Table VIII in Appendix). For MNIST, we follow the architecture given in the Iterative Optimization paper [9]. For Fashion-MNIST and CIFAR-10, we use the WRN-28-10 instantiation of the wide residual networks [21].

Here we give a brief description on how the nine schemes are different from each other, and the values chosen for their specific training parameters. The main principle behind choosing such parameters is that we want to make the resulting models to all have a comparable level of test error. We first begin with the schemes that do not involve adversarial training, and then we discuss how adversarial examples were generated for training purposes, and then describe the schemes that use adversarial training. For each scheme, we train 16 models (which are shadows of each other) on each dataset, and present the mean and standard deviation of test accuracy in Table I.

1) **Normal Training:** Here we describe the 7 training schemes that do not use adversarial training.

a) **Standard:** The baseline models we consider in this paper simply follow the architectures given in Table VII using the parameters shown in Table VIII, and they do not use any

TABLE I: Test error (mean \pm std) of each scheme. The statistics were calculated based on the 16 models trained for each scheme on each dataset.

		MNIST	Fashion-MNIST	CIFAR-10
Standard		$0.77 \pm 0.05\%$	$4.94 \pm 0.19\%$	$4.38 \pm 0.21\%$
Dropout	Single pred.	$0.63 \pm 0.08\%$	$4.88 \pm 0.14\%$	$4.53 \pm 0.30\%$
Distillation	Single pred.	$0.74 \pm 0.06\%$	$4.96 \pm 0.19\%$	$4.43 \pm 0.29\%$
RS-1	Single pred.	$0.93 \pm 0.12\%$	$5.44 \pm 0.12\%$	$5.69 \pm 0.23\%$
RS-1-Dropout	Single pred.	$1.09 \pm 0.62\%$	$5.41 \pm 0.15\%$	$6.05 \pm 0.33\%$
RS-1-Adv	Single pred.	$1.24 \pm 0.39\%$	$5.57 \pm 0.15\%$	$6.25 \pm 0.38\%$
Magnet	<i>Det. Thrs.</i>	0.001	0.004	0.004
	Single pred.	$0.84 \pm 0.08\%$	$5.49 \pm 0.17\%$	$5.59 \pm 0.27\%$
Dropout-Adv	Single pred.	$0.69 \pm 0.08\%$	$4.84 \pm 0.12\%$	$4.75 \pm 0.17\%$
RC	<i>L2 noise</i>	0.4	0.02	0.02
	Voting	$0.77 \pm 0.11\%$	$5.39 \pm 0.23\%$	$5.72 \pm 0.46\%$

randomized algorithms (e.g., Dropout and Random Spiking) or defense mechanisms.

b) **Dropout:** For MNIST, we use replacement probability $1 - p = 0.5$, and the placement of the additional Dropout layer is between the 2 Dense.ReLU layers (see Table VII in Appendix). For Fashion-MNIST and CIFAR-10, we use replacement probability $1 - p = 0.1$, and we follow the “wide-dropout” residual block design described in [21].

c) **Magnet:** We use the trained *Dropout* model as the prediction model, and train the Magnet defensive models (reformers and detectors) [4] based on the publicly released Magnet implementation¹. The network architecture and training parameters we used for the defensive models are identical to those of the original paper.

When evaluating on the test images, we use a set of detectors and a reformer together with the prediction (*Dropout*) model. For Fashion-MNIST and CIFAR-10, we use Reformer II, Detector II/ L_1 , Detector II/ T_{10} and Detector II/ T_{40} , which are consistent with the settings presented in the original paper [4], though for the detection threshold (rate of false positive, noted as *Det. Thrs.* in Table I), we use a smaller threshold of 0.004, so that the model utility increases and the test error becomes comparable to that of the other schemes. For MNIST, we use Reformer I, Detector I/ L_2 and Detector II/ L_1 , detection threshold set to 0.001, which are the same² as the settings presented in the original Magnet paper [4].

d) **Random Spiking with standard model (RS-1):** This is the training scheme where we add a Random Spiking (RS) layer after the first convolution layer in the *standard* architecture. We choose $p = 0.8$, which implies 20% of all neuron outputs are being randomly spiked. We chose 20% so that the training will experience adequate amount of noise, but the network can still converge with SGD. We leave the evaluation on the effect of other values of p for future research.

The RS layer is placed after ReLU activation. Otherwise, ReLU activation would mute negative noises if RS is applied before ReLU, which will make the amount of noise less than

¹<https://github.com/Trevillie/MagNet>

² Regarding the Detector settings, a small discrepancy exists between the paper and the released source code. After confirming with the authors, we follow what is given by the source code.

1– p . We put RS layer after the first convolution layer, because: 1) For MNIST, the network does not converge if we put the RS layer after some later convolution layers; 2) in our preliminary experiments, this gave a slightly better test accuracy.

e) Random Spiking with Dropout (RS-I-Dropout): Instead of the standard scheme, we add the RS layer to the *Dropout* scheme. All other parameters are identical to what we used for RS-I.

f) Distillation: We use the same network architecture and parameters as we did for the training of *Dropout* models. For all three datasets, we train the distillation model with temperature $T = 100$ and test with $T = 1$, which are identical to the configuration used in [9].

g) Region-based Classification (RC): We use the trained *Dropout* models for RC [3]. For each test example, we generate t additional examples, where for each pixel, a noise was randomly chosen from $(-r, r)$ and added to it. Prediction is then made with majority voting on the t input examples. For MNIST, we use $t = 10,000$ and $r = 0.4$. For Fashion-MNIST and CIFAR-10, we use $t = 1,000$ and $r = 0.02$.

2) Adversarial examples and amount of perturbation:

Now we discuss how to generate adversarial examples that are useful for both training purposes and robustness evaluations.

a) Generating Adversarial Examples: For each of the first 6 training schemes discussed previously, we randomly choose 2 out of the 16 shadow models trained and apply the Iterative Optimization L_2 targeted attack on them. For MNIST, we use the first 200 images with confidence values $\{0, 5, 10, 15, 20, 30\}$. For Fashion-MNIST, we use the first 50 images with confidence values $\{0, 20, 40, 60, 70\}$. For CIFAR-10, we use the first 50 images with confidence value $\{0, 20, 40, 60, 80, 100, 120, 140\}$.

Since RC introduces random noise and adds significant overhead in inference comparing to other scheme, it is impractical to directly attack RC. Instead, we use adversarial examples generated on the *Dropout* models, which is the core prediction model used in our setup of RC.

When attacking the Magnet models, we increase the detector’s detection threshold to obtain adversarial examples that are more likely to be transferable. For MNIST and CIFAR-10, we multiply the *Det. Thrs.* in Table I by 10. For Fashion-MNIST, we multiply the *Det. Thrs.* in Table I by 5.

To attack the Distillation models, we found that one needs to use higher confidence values to compensate for the effect of temperature $T = 100$ on the logits. For MNIST, we multiple the confidence values presented above with 100. For Fashion-MNIST and CIFAR-10, we increase the confidence values by a factor of 40, as our preliminary experiments suggest that making the confidence value even higher would significantly reduce the attack success rate.

b) Upper Bounds on Perturbation: For each dataset, we generated thousands of adversarial examples for each training scheme, and have them sorted according to the added amount of perturbation, measured in L_2 . We then empirically approximated a common cut-off upper bound on L_2 distance for all the training schemes, where the generated examples would start to

TABLE II: Adversarial Training Parameters. The values for k were chosen so that the generated examples would fit a L_2 cut-off, determined empirically based on human perception.

Dataset	L_2 cut-off	Working confidence values (k)	Samples for each k (n)
MNIST	3.25	$\{0, 5, 10, 15\}$	3000
Fashion-MNIST	2.0	$\{0, 20, 40, 60\}$	3000
CIFAR-10	2.0	$\{0, 20, 40, 60, 80, 100\}$	2000

look noticeably different under human perception. These L_2 cut-off bounds are reported in Table II, and are used as the upper limits in many of our later experiments.

3) Adversarial training: With the bounds on L_2 fixed, we then empirically determine an upper bound for the confidence value to be used in the Iterative Optimization- L_2 attacks for generating adversarial examples for training purposes. To diversify the set of generated adversarial examples, we sample several different confidence values within the bound, which are also reported in Table II. Now we describe the remaining 2 adversarial training methods

a) Adversarial Dropout (Dropout-Adv): To use adversarial training with *Dropout*, we leverage the trained Dropout model from before as the target model for generating adversarial examples. As described in Table II, for each target model and a given confidence value k , we randomly sample n pairs of (training example, target label) to apply the Iterative Optimization- L_2 targeted attack. We generated 12,000 adversarial examples for each *Dropout* model. To keep a large safe margin, we further sort the adversarial examples according to their L_2 distances in ascending order, and add only the first 10,000 examples into the training dataset, and manually verified that the perturbation done on them do not affect classification under human perception. We then apply the Dropout training procedure as described before on the new training dataset.

b) Adversarial Random Spiking (RS-I-Adv): For this adversarial training method, we use RS-I as the target model. The training parameters and procedure are largely identical to what were described for Dropout-Adv above, summarized in Table II, except that for Fashion-MNIST, we use an alternative confidence value set of $\{0, 20, 40, 50\}$. This is because when $k \geq 60$, we found that it is not always possible to find adversarial examples (success rate drops significantly), and some of the examples generated have noticeable differences when compared to the benign ones.

B. Applying Bagging and Randomness in Inference

We note that there are techniques that can be used during prediction to improve test accuracy and model robustness. Bagging, for example, is one such technique that uses multiple models. Given N models that share identical architecture, bagging can be used during prediction by computing

$$C(x) = \arg_i \max \left(\text{softmax} \left(\sum_{i=1}^N Z_i(x) \right) \right)$$

where $Z_i(x)$ is the output before the softmax layer, and

TABLE III: Test error (mean \pm std) of each scheme. The statistics were calculated based on the 16 models trained for each scheme on each dataset. When Bagging is applicable, it generally performs better than voting.

		MNIST	Fashion-MNIST	CIFAR-10
Standard		0.77 \pm 0.05%	4.94 \pm 0.19%	4.38 \pm 0.21%
Dropout	Voting	0.66 \pm 0.08%	4.77 \pm 0.10%	4.49 \pm 0.25%
	Bagging	0.65 \pm 0.08%	4.76 \pm 0.11%	4.47 \pm 0.27%
Distillation	Voting	0.78 \pm 0.06%	4.82 \pm 0.17%	4.32 \pm 0.26%
	Bagging	0.77 \pm 0.05%	4.81 \pm 0.16%	4.33 \pm 0.28%
RS-1	Voting	0.86 \pm 0.09%	5.35 \pm 0.12%	5.60 \pm 0.20%
	Bagging	0.87 \pm 0.08%	5.36 \pm 0.13%	5.59 \pm 0.23%
RS-1-Dropout	Voting	0.73 \pm 0.08%	5.32 \pm 0.18%	5.84 \pm 0.43%
	Bagging	0.71 \pm 0.08%	5.31 \pm 0.16%	5.84 \pm 0.25%
RS-1-Adv	Voting	1.00 \pm 0.11%	5.50 \pm 0.13%	6.21 \pm 0.40%
	Bagging	0.97 \pm 0.09%	5.49 \pm 0.17%	6.23 \pm 0.40%
Magnet	<i>Det Thrs</i>	0.001	0.004	0.004
	Voting	0.88 \pm 0.08%	5.38 \pm 0.15%	5.56 \pm 0.22%
	Bagging	0.88 \pm 0.06%	5.39 \pm 0.15%	5.52 \pm 0.24%
Dropout-Adv	Voting	0.72 \pm 0.10%	4.79 \pm 0.11%	4.73 \pm 0.20%
	Bagging	0.70 \pm 0.09%	4.77 \pm 0.10%	4.74 \pm 0.20%
RC	<i>L₂ noise</i>	0.4	0.02	0.02
	Voting	0.77 \pm 0.11%	5.39 \pm 0.23%	5.72 \pm 0.46%

$i \in [1, N]$. Recall the softmax function defined in Section II, bagging can sometimes smoothen outputs of the softmax layer.

Furthermore, we note that randomized algorithms such as Dropout and Random Spiking are not only applicable to the training phase, but can also be used during prediction. In the latter case, for each input, one can get multiple randomized outputs of $Z(x)$ with one trained model through repeated predictions. Those different outputs can then be aggregated into a single output through *majority voting* or *bagging*.

We empirically found that in many cases, applying Dropout or Random Spiking and then bagging can slightly improve test accuracy. The results can be found in Table III. For *Voting*, each model performs 10 predictions on a given input, with Dropout or Random Spiking if one of the two was used during training. The final prediction is then picked based on majority vote. Prediction with *Bagging* performs similarly but instead of majority vote, the bagging computation described above is used. Results in Table III show that *Bagging* performs the best in many case. Also, *Bagging* gives smaller standard deviations on test error, which implies the models perform more robustly. Also notice that the test errors of various defense methods are still within comparable range. Given the improvements on test accuracy, for later experiments, we will use single prediction for standard, voting for RC as mandated by its design, and bagging (with Dropout or Random Spiking if used in training) for the remaining schemes.

C. Evaluating Model Stability

Given an original benign image and its variants with added noise, a more robust model should intuitively be able to tolerate a higher level of noise without changing its prediction results. We refer to this property as model stability. We believe that the stability of a model correlates with its resistance to adversarial examples. In other words, higher model stability

TABLE IV: Average L_2 distance (\pm std. dev.) between two images of same/different label in the training datasets

	MNIST	Fashion-MNIST	CIFAR-10
Same Label	8.92 \pm 1.81	8.72 \pm 2.49	18.26 \pm 4.62
Different Label	10.30 \pm 1.31	11.67 \pm 2.51	19.05 \pm 4.54

suggests higher model robustness. Here we measure model stability through the following two experiments.

1) **Gaussian Noise Resistance:** Given a set of benign images, we measure how many predictions would change if a fixed amount of Gaussian noise is introduced to the images. For a given dataset and a model, we use the first 1,000 images from the test dataset. We first make a prediction on those selected images and store the results as *reference predictions*. Then, for each benign image selected and a chosen L_2 distance, we sample Gaussian noise, scale it to the desired L_2 value, and add the noise to the image. Pixel values are clipped if necessary, to make sure the new noisy variant is a valid image. We repeat this process 20 times (noise sampled independently per iteration). For the sake of time efficiency, for this particular set of experiments, we reduced the number of iterations used by RC to one-tenth of its original algorithm.

The effect of Gaussian noise on prediction accuracy for each training method (averaged over the 16 models trained) can be found in Fig. 1. In addition to prediction accuracy, we also measured the percentage of predictions that remained the same when noise is introduced, the result of which can also be found in Fig. 1. For MNIST, we stopped the experiments after the L_2 distance is more than half of the average distance among images in the training dataset that share the same labels, shown in Table IV. For Fashion-MNIST and CIFAR-10, we stopped the experiments after the trained models start to experience significant decreases in prediction accuracy and stability.

Model stability (in terms of both prediction accuracy and stability) inevitably drops for each scheme as the amount of Gaussian noise increases. Overall, the RS-class models generally give more accurate and stable predictions than the others under the same amount of noise. Among the 16 models trained for each scheme, the RS-class ones also tend to have smaller standard deviations in the prediction accuracy and stability measurements, which is another evidence suggesting higher model stability.

Under a relatively higher amount of noise, the RS-class models performed the best on the CIFAR-10 dataset. For Fashion-MNIST, the models from adversarial training (*i.e.*, RS-1-Adv and Dropout-Adv) stood out, followed by the rest of the RS-class models. The results on MNIST are somewhat mixed, but as the amount of noise increases, prediction accuracy and stability of the RS-class models tend to decrease slower than the others.

Since randomness is applied in inference through bagging as discussed in Section V-B, the percentage of unchanged predictions is slightly lower than 100% even if no noise is introduced, except for the standard models.

2) **Random Walk:** Here we present more fine-grained measurements of prediction stability under increasing amounts

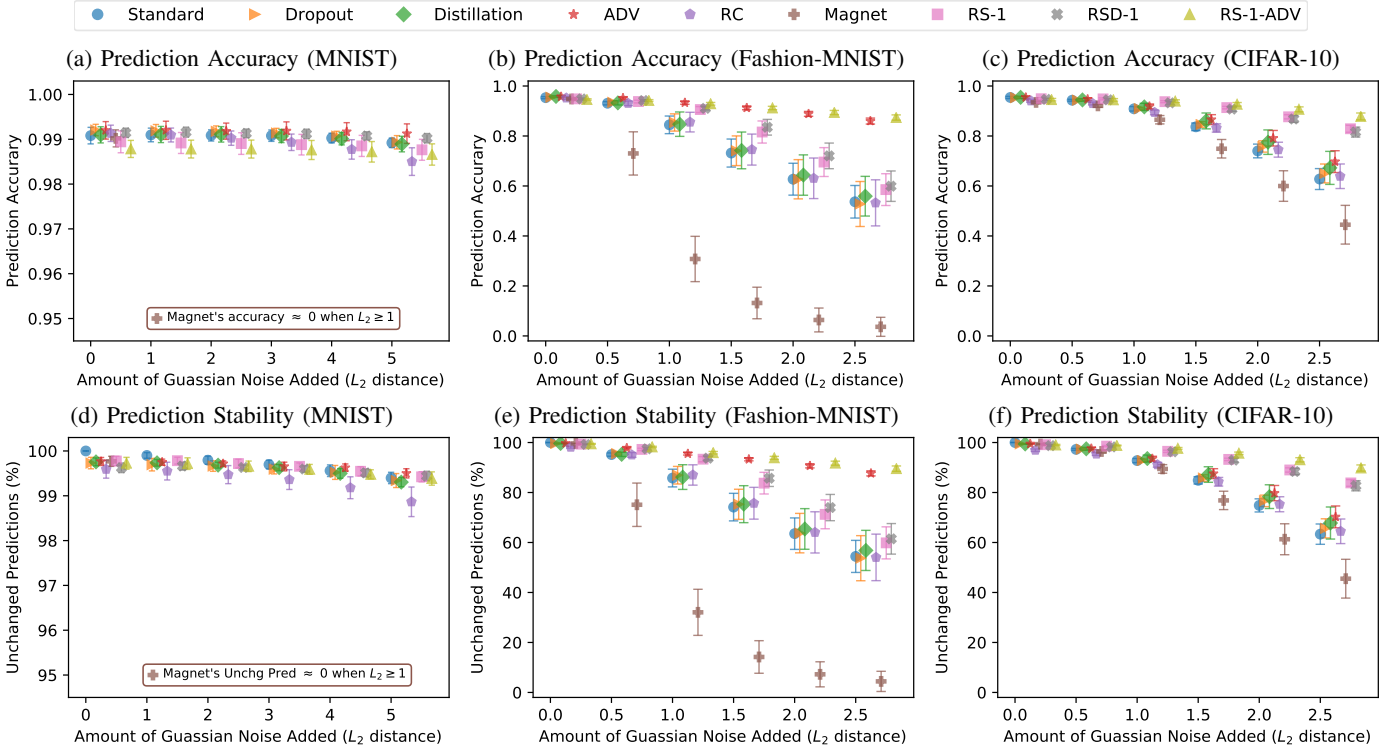


Fig. 1: Evaluating model stability with Gaussian Noise

of Gaussian noise. Given an original image x_0 , we iteratively add a fixed amount of Gaussian noise to x_i to generate a new image x_{i+1} in step i . To make sure the newly generated image is still valid, we flip the sign of noise and clip pixel values if necessary. We then count the number of prediction changes as the steps proceed. A change is recorded if the prediction on x_i and x_{i+1} are different. We run 50 steps for each of the first 1,000 images in each of the datasets. The incremental step size in terms of L_2 is 0.4 for all three datasets. Other parameters are the same as in the experiment on Gaussian Noise Resistance discussed above. We summarize the results in Table V. The first and second columns show that after the i -th step of the random walk experiment, the average amount of noise being added to the benign images, measured in L_2 . The remaining columns show the average number of prediction changes for each model, after certain steps of random walk.

For MNIST, most models exhibit comparable levels of prediction stability, similar to the results shown in Fig. 1. This could be attributed to the fact that images in this dataset are relatively simple with only grayscale pixels, hence to some extent the dataset itself is noise resistant. For Fashion-MNIST and CIFAR-10, the adversarially trained ones have the best stability, in which RS-1-Adv performs better than Dropout-Adv. They are followed by the remaining RS-class models, where RS-1 performs better than RS-1-Dropout. The relative stability of Magnet on MNIST and Fashion-MNIST is mostly due to many examples being rejected by the detectors, hence the stable behaviors, but low utility. The Magnet detectors seem to fluctuate when random walking the CIFAR-10 dataset, hence the higher number of prediction changes.

D. Evaluating Attack Strategies

Here we empirically show that our proposed attack strategy, as presented in Section III-C, can indeed generate adversarial examples that are more transferable. Transferability is an important property, especially in the translucent-box setting, as an attacker can leverage shadow models to generate adversarial examples to try and attack the target model. In attacks like the Iterative Optimization attack, a higher confidence value will typically lead to more transferable examples, but the amount of perturbation would usually increase as well, sometimes making the example noticeably different under human perception.

This however gives us a metric for evaluating attack strategies. Intuitively, a better attack strategy should give more transferable adversarial examples using less amount of distortion. Hence we use *Distortion vs Transferability* to compare 3 possible attack strategies. Similar to previous experiments, we measure the amount of distortion using L_2 distance. The detailed results can be found in Fig. 4 in Appendix.

The first strategy we evaluate is a typical Iterative Optimization attack which generates adversarial examples using only one shadow model, dubbed ‘Single’. Recall that for each training/defense method, we have 16 models that are shadows of each other (Section V-A). For the *Single* strategy, we apply the Iterative Optimization attack on 2 of the models independently to generate a pool of adversary examples. The transferability of those examples are then measured and averaged on the remaining 14 target models. Regardless of the training methods and defense mechanisms in place, adversarial examples generated using the *Single* strategy often have limited transferability,

TABLE V: Average number of prediction changes under the Random Walk experiment

Step	L_2	Standard	Dropout	Distillation	Dropout-Adv	RC	Magnet	RS-1	RS-1-Dropout	RS-1-Adv
10	1.45±0.03	0.00±0.11	0.02±0.29	0.02±0.29	0.02±0.27	0.01±0.12	1.00±0.05	0.02±0.26	0.03±0.35	0.02±0.29
20	2.00±0.05	0.01±0.18	0.04±0.53	0.04±0.55	0.04±0.52	0.01±0.23	1.00±0.05	0.04±0.50	0.06±0.66	0.04±0.55
30	2.41±0.06	0.01±0.24	0.06±0.77	0.07±0.81	0.05±0.75	0.02±0.32	1.00±0.05	0.06±0.73	0.08±0.97	0.06±0.79
40	2.75±0.06	0.02±0.31	0.08±1.01	0.09±1.06	0.07±0.97	0.03±0.42	1.00±0.05	0.08±0.97	0.12±1.28	0.08±1.02
50	3.05±0.07	0.02±0.37	0.10±1.25	0.12±1.32	0.09±1.19	0.03±0.50	1.00±0.05	0.10±1.20	0.15±1.59	0.11±1.25

(a) MNIST, $L_2 = 0.4$ in each step

Step	L_2	Standard	Dropout	Distillation	Dropout-Adv	RC	Magnet	RS-1	RS-1-Dropout	RS-1-Adv
10	1.38±0.05	0.76±1.21	0.68±1.17	0.66±1.20	0.17±0.67	0.57±1.03	1.06±0.48	0.36±0.86	0.36±0.88	0.14±0.60
20	1.90±0.06	1.63±2.09	1.56±2.08	1.55±2.17	0.38±1.19	1.32±1.83	1.18±0.85	0.97±1.64	1.06±1.74	0.29±1.06
30	2.29±0.08	2.44±2.81	2.42±2.85	2.44±2.99	0.66±1.71	2.05±2.52	1.36±1.30	1.66±2.34	1.84±2.49	0.48±1.53
40	2.62±0.09	3.19±3.45	3.23±3.54	3.31±3.72	1.06±2.27	2.76±3.14	1.59±1.81	2.37±3.00	2.68±3.19	0.70±2.01
50	2.91±0.10	3.89±4.03	3.99±4.18	4.15±4.39	1.57±2.84	3.41±3.70	1.89±2.33	3.08±3.62	3.53±3.87	0.96±2.50

(b) Fashion-MNIST, $L_2 = 0.4$ in each step

Step	L_2	Standard	Dropout	Distillation	Dropout-Adv	RC	Magnet	RS-1	RS-1-Dropout	RS-1-Adv
10	1.26±0.02	0.22±0.70	0.22±0.74	0.20±0.70	0.19±0.69	0.19±0.65	0.34±0.87	0.14±0.64	0.17±0.74	0.12±0.65
20	1.78±0.03	0.54±1.28	0.56±1.38	0.51±1.31	0.49±1.30	0.49±1.21	0.88±1.58	0.33±1.19	0.41±1.39	0.28±1.17
30	2.17±0.04	0.93±1.83	1.00±2.02	0.90±1.92	0.86±1.89	0.85±1.75	1.51±2.20	0.59±1.78	0.72±2.06	0.46±1.68
40	2.50±0.05	1.37±2.37	1.50±2.63	1.37±2.52	1.30±2.49	1.26±2.25	2.15±2.76	0.91±2.40	1.10±2.75	0.67±2.21
50	2.79±0.06	1.85±2.86	2.07±3.22	1.89±3.10	1.79±3.06	1.71±2.71	2.79±3.28	1.29±3.04	1.54±3.47	0.93±2.75

(c) CIFAR-10, $L_2 = 0.4$ in each step

especially when the allowed amount of distortion (L_2 distance) is small (see Fig. 4 in Appendix).

The second attack strategy that we evaluate is to generate adversarial examples using multiple shadow models. For this, we use 8 of the 16 shadow models for generating attack examples. The Iterative Optimization attack can be adapted to handle this case with a slightly different loss function. In our experiments, we use the sum of the loss functions of the 8 shadow models as the new loss function. We also use slightly lower confidence values than in Section V-A2 ($\{0, 10, 20, 30, 40\}$ for Fashion-MNIST, $\{0, 20, 40, 60, 80\}$ CIFAR-10). The transferability of the generated adversarial examples are then measured and averaged on the remaining 8 models as the target. We refer to this as ‘*Multi 8*’. This is a realistic attack strategy in the translucent-box setting, as an adversary with enough knowledge and time can easily train multiple shadows in attempt to generate high quality adversarial examples that are more likely to trick the target. Given the same limit on the amount of distortion (L_2 distance), a significantly higher percentage of examples generated using the *Multi 8* strategy are transferable than those found using the *Single* strategy (see Fig. 4 in Appendix).

Additionally, we evaluate a third attack strategy that is based on *Multi 8*. As discussed in Section III-C, given enough shadow models, one can further use some of them for validating adversarial examples. This validation process can be viewed as a sieve of adversarial examples, so that only those with high likelihood of tricking the target model would be used in the actual attack. This is particularly useful if the target model is behind some protection mechanisms that rate limit query access to the model (e.g., in a cloud setting). In our experiments, similar to the *Multi 8* strategy, we leverage 8 shadow models to generate adversarial examples using the Iterative Optimization attack. Furthermore, we use 7 of the remaining 8 models for validation. Adversarial examples are

kept only if they can be transferred to at least 5 of the 7 validation models, hence we refer to this strategy *Multi 8 & Passing 5/7 Validation*. The remaining model is used as the attack target, and we measure the transferability of examples that passed the *5/7 Validation*. The measurements shown in Fig. 4 is the average of 8 rotations of target model and validation models. Comparing to *Multi 8* and *Single*, adversarial examples that passed the *5/7 Validation* are significantly more likely to be able to transfer to the target model, especially when the amount of perturbation is small.

This shows that simple strategies like *Single* are indeed not realizing the full potential of a resourceful attacker, and our proposed attack strategy of using multiple models for generation and validation of adversarial examples is indeed superior. In the rest of this section, we will be focusing on the attack strategy of *Multi 8 & Passing 5/7 Validation*.

E. White-box Evaluation

As a preliminary evaluation of defense mechanisms, one can apply the Iterative Optimization white-box attack to generate targeted adversarial examples as discussed before. Given a larger confidence value k used in such attacks, the adversarial examples generated tend to have a larger L_2 distance (more distorted). Intuitively, for each fixed value of k , if a trained model is more robust, the adversarial examples found by the Iterative Optimization attack should have a larger L_2 distance than the other models.

We compare the L_2 distance of the adversarial examples generated using the *Multi 8* attack strategy, under different confidence values for the trained models (introduced in Section V-B). For each (model, confidence value) pair, we apply the Iterative Optimization attack to generate 1,800 adversarial examples for MNIST, and 450 adversarial examples for Fashion-MNIST and CIFAR-10. In Fig. 2 we present the average L_2 distance of the generated examples under a chosen confidence value, as well the CDF of the L_2 distance

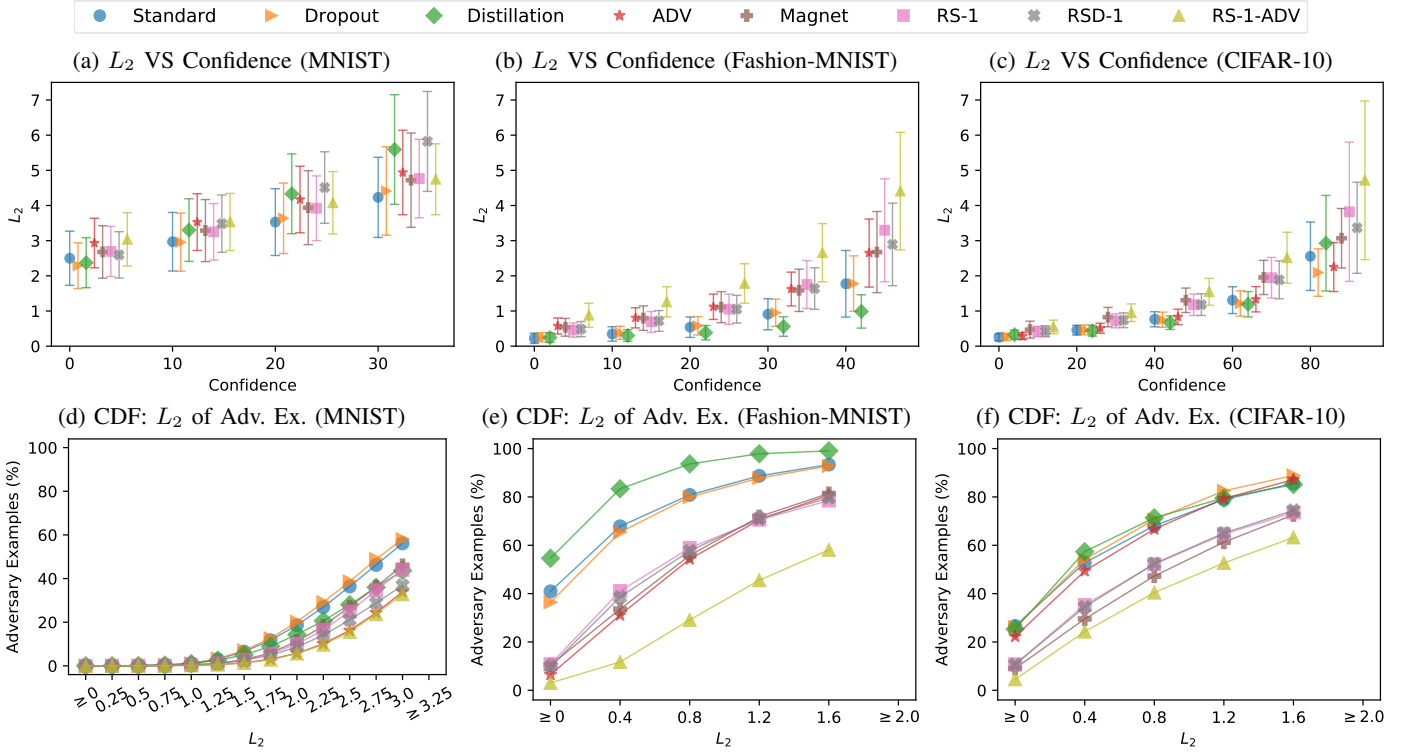


Fig. 2: L_2 distance of adversarial examples found by the *Multi 8* attack strategy. The 3 subfigures on the bottom illustrate the CDF of the L_2 distance of the generated adversarial examples.

of all the generated examples considered valid, based on the L_2 cut-off presented in Table II. As shown in Fig. 2, for Fashion-MNIST and CIFAR-10, RS-1-Adv requires on average more perturbations (measured in L_2 distance) than the other models under the same confidence value, and the percentage of valid examples that use small perturbations is also smaller. For MNIST, the results are somewhat mixed, but both RS-class models and adversarially trained models showed their merits, especially over the standard and dropout models. These suggest that the RS-class defenses can indeed increase model robustness against adversarial examples.

F. Translucent-box Evaluation

As discussed before, transferability is of particular interest under the Knowledge of Process (translucent-box) setting. Here we evaluate the robustness of different models based on how many adversarial examples (generated based on shadows and other models trained/equipped with different defense mechanisms) can be transferred to work against them. For this we use the *Multi 8* & *Passing 5/7 Validation* attack strategy. That is, recall that for each scheme, we have trained 16 models that are shadows of each other. We use 8 models for generating adversarial examples, and use 7 of the remaining 8 for validation purposes. A targeted adversarial example is deemed valid if it manages to fool at least 5 of the 7 validation models. Our previous experiments (Section V-D) showed that examples passing the *5/7 Validation* have a high chance of being transferable to the actual target model.

TABLE VI: Best attack for each evaluation attack

	Standard	Dropout	Distillation	Dropout-Adv	RC
MNIST	Standard	RS-1	RS-1	Dropout-Adv	Dropout-Adv
Fashion-MNIST	Dropout	Magnet	Dropout	Dropout-Adv	Magnet
CIFAR-10	Magnet	Magnet	Dropout	Dropout-Adv	Magnet
	Magnet	RS-1	RS-1-Dropout	RS-1-Adv	
MNIST	Magnet	RS-1-Adv	RS-1-Adv	RS-1-Adv	
Fashion-MNIST	Magnet	RS-1	RS-1-Adv	RS-1-Adv	
CIFAR-10	Magnet	RS-1-Adv	RS-1-Adv	RS-1-Adv	

Intuitively, the lower the number of adversarial examples that can pass the *5/7 Validation* with models of a particular scheme, the more difficult it is to attack said scheme. We hence evaluate model robustness based on the validation passing rate of each scheme under different L_2 allowance, with adversarial examples generated using 1) shadow models of the target model itself (dubbed “*self*”); and 2) the best of all possible schemes that we have (dubbed “*best*”). We make such a distinction because, interestingly, depending on the scheme used in the actual target model, the Iterative Optimization attack does not necessarily work the best with shadow models that are of the same scheme. In some cases, adversarial examples that are generated using models of other schemes might exhibit higher transferability. The best scheme to generate adversarial examples for each target scheme, determined based on our experiments, can be found in Table VI.

The results of our translucent-box evaluation are shown in Fig. 3. Adversarial examples are grouped into buckets based on their L_2 distance. For each bucket, we plot the average validation passing rate for each scheme. L_2 upper bounds

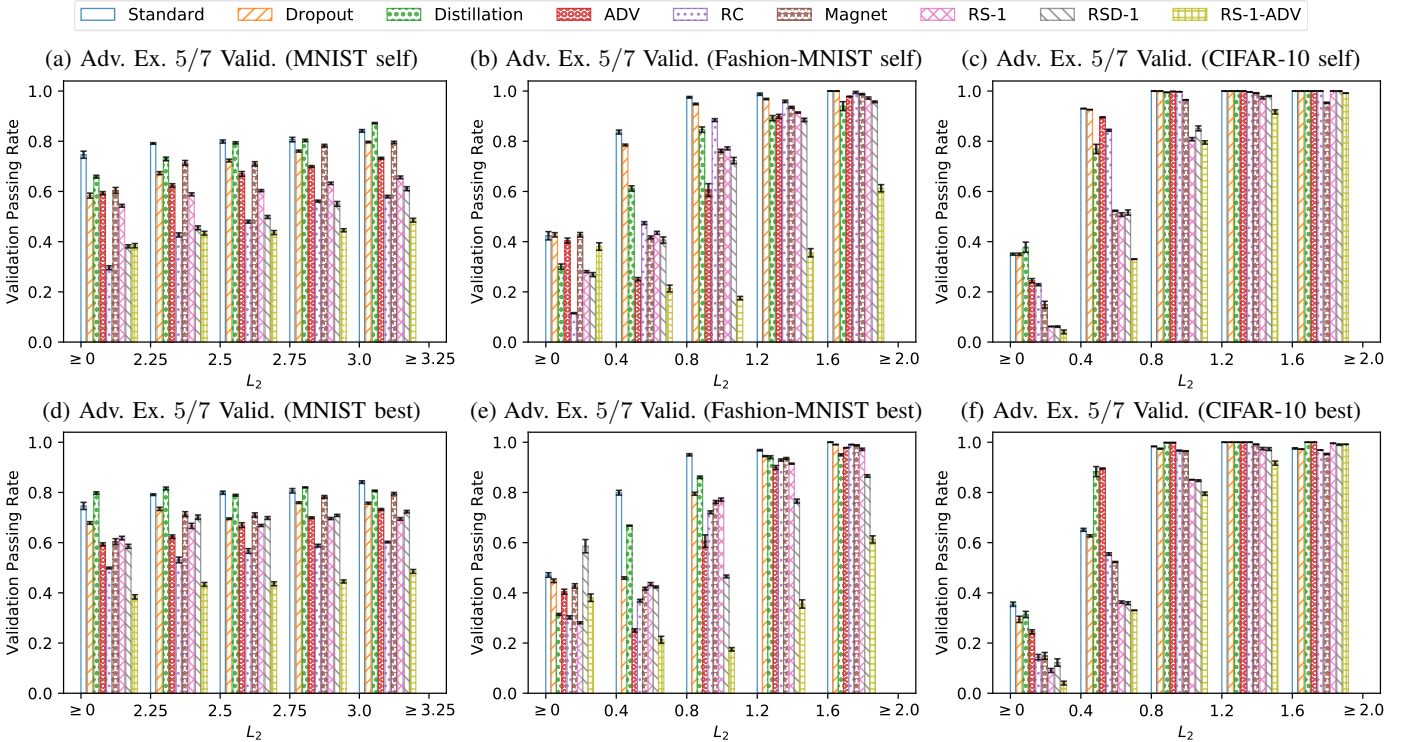


Fig. 3: Translucent-box evaluation with 5/7 Validation passing rate

follow from Table II. A detailed heat map of the average 5/7 *Validation* passing rates for each pair of (generation, target) schemes can be found in Fig. 5–7 in the Appendix.

As explained by Fig. 2, only a small fraction of adversarial examples generated have small L_2 . For most of the buckets, we have at least 100 adversarial examples, and the buckets representing larger L_2 tend to contain more examples.

Overall, across the three datasets, RS-1-Adv performs the best, especially when we increase the L_2 allowance (enabling more perturbations). RS-1 and RS-1-Dropout also perform consistently well across the three datasets. RC performs noticeably well on MNIST and Fashion-MNIST, likely because the images were all in 8-bit grayscale, and its advantages diminish on CIFAR-10 which contains images of 24-bit color.

VI. RELATED WORK

Other attack algorithms. There are other attack algorithms such as JSMA [7], FGS [2], and DeepFool [10]. The general consensus seems to be that the CW attack is the state of the art [9], [22]. Our evaluation framework is not tied to a particular attack and can use other algorithms. Our evaluation results are based on the CW attack.

Other defense mechanisms. Many other defense mechanisms have been proposed [14], [4], [3], [5], [23]. Specifically, Xu *et al.* proposed feature squeezing which detects the adversarial examples with image preprocessing methods such as color bit depths reduction and pixel spatial smoothing [5]. Xie *et al.* proposed image preprocessing with random resizing and padding to defense against adversarial examples. Due to limit in time and space, we selected representative methods from

each broad class, using MagNet for the detection approach. We leave the comparison with these mechanisms for future work.

Beyond images. Other research efforts have explored possible attacks against neural network models specialized for other purposes, for example, speech to text [24]. We focus on images, although the evaluation methodology and the idea of random spiking may be applicable to these other domains.

Alternative similarity metrics. Some researchers have argued that L_p norms insufficiently capture human perception, and have proposed to use alternative similarity metrics like SSIM [8]. It is however, not immediately clear how to adapt such metrics in the Iterative Optimization attack. We leave further investigations on the impacts of alternative similarity metrics on adversarial examples for future work.

VII. CONCLUSION

In this paper, we present a careful analysis of possible adversarial models for studying the phenomenon of adversarial examples. We propose an evaluation methodology that can better illustrate the strengths and limitations of different mechanisms. As part of the method, we introduce a more powerful and meaningful adversary strategy. We also introduced Random Spiking, a randomized technique that generalizes dropout. We have conducted extensive evaluation of Random Spiking and several other defense mechanisms, and demonstrate that Random Spiking, especially when combined with adversarial training, offers better protection against adversarial examples when compared with other existing defenses.

REFERENCES

- [1] C. Szegedy, W. Zaremba, I. Sutskever, J. Bruna, D. Erhan, I. Goodfellow, and R. Fergus, “Intriguing properties of neural networks,” in *International Conference on Learning Representations*, 2014.
- [2] I. Goodfellow, J. Shlens, and C. Szegedy, “Explaining and harnessing adversarial examples,” in *International Conference on Learning Representations*, 2015.
- [3] X. Cao and N. Z. Gong, “Mitigating evasion attacks to deep neural networks via region-based classification,” in *Proceedings of the 33rd Annual Computer Security Applications Conference*. ACM, 2017, pp. 278–287.
- [4] D. Meng and H. Chen, “Magnet: a two-pronged defense against adversarial examples,” in *Proceedings of the 2017 ACM SIGSAC Conference on Computer and Communications Security*. ACM, 2017, pp. 135–147.
- [5] W. Xu, D. Evans, and Y. Qi, “Feature squeezing: Detecting adversarial examples in deep neural networks,” *Network and Distributed Systems Security Symposium*, 2018.
- [6] N. Srivastava, G. Hinton, A. Krizhevsky, I. Sutskever, and R. Salakhutdinov, “Dropout: a simple way to prevent neural networks from overfitting,” *The Journal of Machine Learning Research*, vol. 15, no. 1, pp. 1929–1958, 2014.
- [7] N. Papernot, P. McDaniel, S. Jha, M. Fredrikson, Z. B. Celik, and A. Swami, “The limitations of deep learning in adversarial settings,” in *2016 IEEE European Symposium on Security and Privacy (EuroS&P)*. IEEE, 2016, pp. 372–387.
- [8] P.-Y. Chen, Y. Sharma, H. Zhang, J. Yi, and C.-J. Hsieh, “Ead: Elastic-net attacks to deep neural networks via adversarial examples,” *AAAI Conference on Artificial Intelligence*, 2018.
- [9] N. Carlini and D. Wagner, “Towards evaluating the robustness of neural networks,” in *2017 IEEE Symposium on Security and Privacy (SP)*. IEEE, 2017, pp. 39–57.
- [10] S.-M. Moosavi-Dezfooli, A. Fawzi, and P. Frossard, “Deepfool: a simple and accurate method to fool deep neural networks,” in *Proceedings of the IEEE Conference on Computer Vision and Pattern Recognition*, 2016, pp. 2574–2582.
- [11] N. Carlini and D. A. Wagner, “MagNet and “Efficient Defenses Against Adversarial Attacks” are Not Robust to Adversarial Examples,” *CoRR*, vol. abs/1711.08478, 2017. [Online]. Available: <http://arxiv.org/abs/1711.08478>
- [12] D. P. Kingma and J. Ba, “Adam: A Method for Stochastic Optimization,” in *International Conference on Learning Representations*, 2015.
- [13] G. Hinton, O. Vinyals, and J. Dean, “Distilling the Knowledge in a Neural Network,” *NIPS 2014 Deep Learning and Representation Learning Workshop*.
- [14] N. Papernot, P. D. McDaniel, X. Wu, S. Jha, and A. Swami, “Distillation as a defense to adversarial perturbations against deep neural networks,” *CoRR*, vol. abs/1511.04508, 2015. [Online]. Available: <http://arxiv.org/abs/1511.04508>
- [15] N. Papernot, P. McDaniel, I. Goodfellow, S. Jha, Z. B. Celik, and A. Swami, “Practical black-box attacks against machine learning,” in *Proceedings of the 2017 Asia Conference on Computer and Communications Security*. ACM, 2017, pp. 506–519.
- [16] P. Vincent, H. Larochelle, Y. Bengio, and P.-A. Manzagol, “Extracting and composing robust features with denoising autoencoders,” in *Proceedings of the 25th International Conference on Machine Learning*. ACM, 2008, pp. 1096–1103.
- [17] P. Vincent, H. Larochelle, I. Lajoie, Y. Bengio, and P.-A. Manzagol, “Stacked denoising autoencoders: Learning useful representations in a deep network with a local denoising criterion,” in *Proceedings of the 27th International Conference on Machine Learning*, vol. 11. JMLR.org, Dec. 2010, pp. 3371–3408.
- [18] Y. LeCun, C. Cortes, and C. J. Burges, “The MNIST database of handwritten digits.” 1998. [Online]. Available: <http://yann.lecun.com/exdb/mnist/>
- [19] H. Xiao, K. Rasul, and R. Vollgraf, “Fashion-MNIST: a Novel Image Dataset for Benchmarking Machine Learning Algorithms,” *CoRR*, vol. abs/1708.07747, 2017. [Online]. Available: <http://arxiv.org/abs/1708.07747>
- [20] A. Krizhevsky, “Learning multiple layers of features from tiny images,” *Tech. Rep.*, 2009.
- [21] S. Zagoruyko and N. Komodakis, “Wide residual networks,” *CoRR*, vol. abs/1605.07146, 2016. [Online]. Available: <http://arxiv.org/abs/1605.07146>
- [22] N. Carlini and D. Wagner, “Adversarial examples are not easily detected: Bypassing ten detection methods,” in *Proceedings of the 10th Workshop on Artificial Intelligence and Security*. ACM, 2017, pp. 3–14.
- [23] C. Xie, J. Wang, Z. Zhang, Z. Ren, and A. L. Yuille, “Mitigating adversarial effects through randomization,” *International Conference on Learning Representations (ICLR)*, 2018.
- [24] N. Carlini and D. Wagner, “Audio Adversarial Examples: Targeted Attacks on Speech-to-Text,” *Deep Learning and Security Workshop*, p. arXiv:1801.01944, 2018.

VIII. APPENDIX

A. Additional Tables and Figures

Here we provide additional details regarding the setup and results of our experiments.

The model architecture and training parameters can be found in Table VII and VIII.

TABLE VII: Model Architecture for the MNIST (identical to the MagNet [4], [9]); Fashion-MNIST and CIFAR-10 (identical to the WRN [21]). In WRN-28-10, where $k = 10$, $N = 4$, we show groups of convolutional layers (kernel 3×3) in brackets where N is the number of blocks in the group, and k is the fraction of number of features.

MNIST		Fashion-MNIST			CIFAR-10		
		Group	Output Size	Kernel, Feature	Output Size	Kernel, Feature	
Conv.ReLU	$3 \times 3 \times 32$						
Conv.ReLU	$3 \times 3 \times 32$	Conv1	28×28	$\begin{bmatrix} 3 \times 3, 16 \end{bmatrix}$	32×32	$\begin{bmatrix} 3 \times 3, 16 \end{bmatrix}$	
Max Pooling	2×2						
Conv.ReLU	$3 \times 3 \times 64$	Conv2	28×28	$\begin{bmatrix} 3 \times 3, 16 \times k \end{bmatrix} \times N$	32×32	$\begin{bmatrix} 3 \times 3, 16 \times k \end{bmatrix} \times N$	
Conv.ReLU	$3 \times 3 \times 64$						
Max Pooling	2×2	Conv3	14×14	$\begin{bmatrix} 3 \times 3, 32 \times k \end{bmatrix} \times N$	16×16	$\begin{bmatrix} 3 \times 3, 32 \times k \end{bmatrix} \times N$	
Dense.ReLU	200						
Dense.ReLU	200	Conv4	7×7	$\begin{bmatrix} 3 \times 3, 64 \times k \end{bmatrix} \times N$	8×8	$\begin{bmatrix} 3 \times 3, 64 \times k \end{bmatrix} \times N$	
Softmax	10	Softmax	10		10		

TABLE VIII: Training Parameter for the MNIST (identical to the MagNet [4], [9]), Fashion-MNIST and CIFAR-10 Models (identical to the WRN [21])

Parameters	MNIST	Fashion-MNIST & CIFAR-10
Optimization Method	SGD	SGD
Learning Rate	0.01	0.1 initial, multiply by 0.2 at 60, 120 and 160 epochs
Momentum	0.9	0.9
Batch Size	128	128
Epochs	50	200
Dropout (Optional)	0.5	0.1
Data Augmentation	-	Fashion-MNIST: Shifting + Horizontal Flip CIFAR-10: Shifting + Rotation + Horizontal Flip + Zooming + Shear

The detailed comparisons of the transferability of adversarial examples generated by the 3 attack strategies can be found in Fig. 4.

A detailed heat map of the average 5/7 Validation passing rates for each pair of (generation, target) schemes can be found in Fig. 5–7.

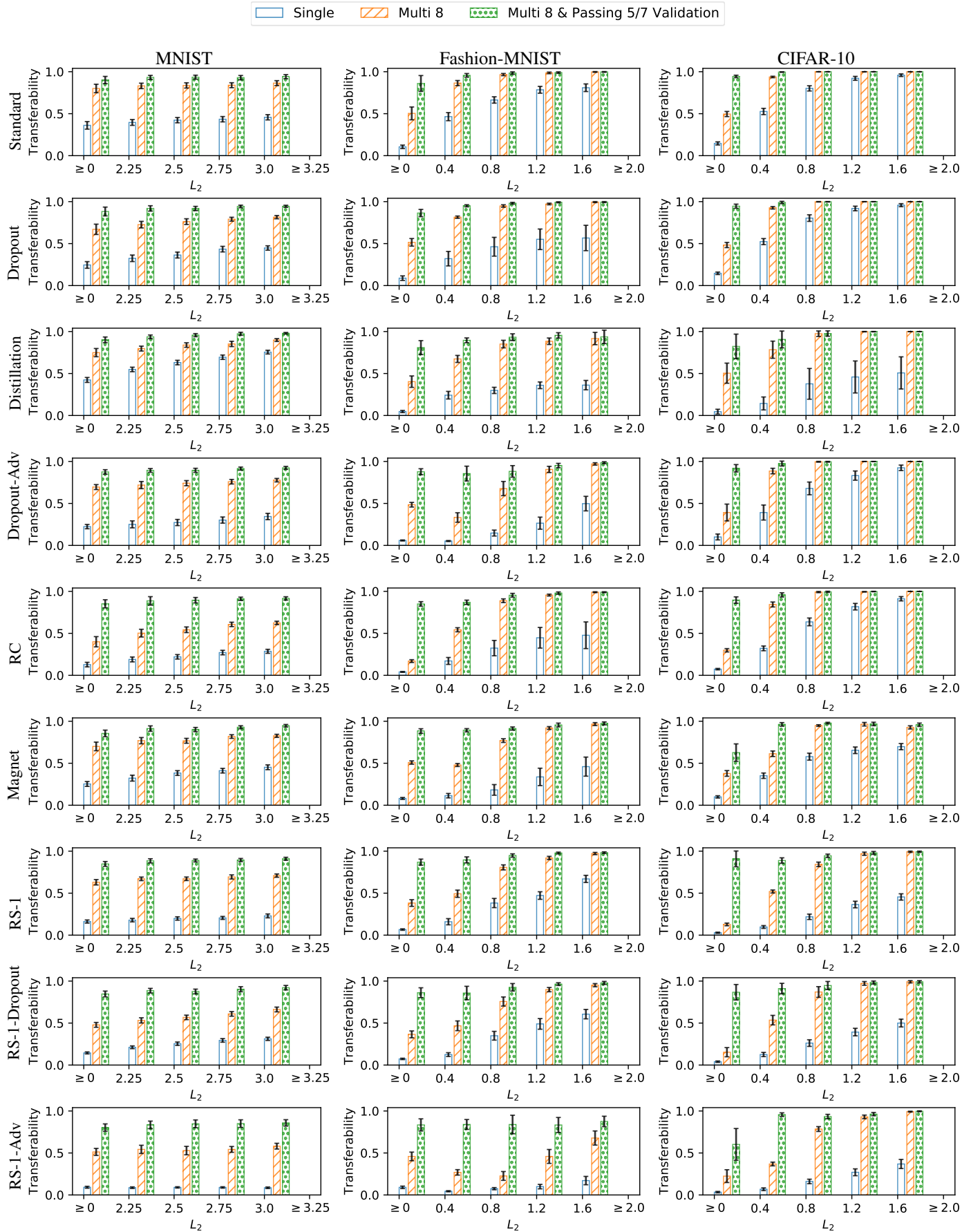


Fig. 4: Transferability of adversarial examples found by the 3 attack strategies

	Standard	Dropout	Distillation	Dropout-Adv	RC	Magnet	RS-1	RS-1-Dropout	RS-1-Adv	All
$L_2 : 0 - 2.25$										
Standard	74.63±1.42	52.75±0.73	72.56±0.40	3.10±0.13	26.92±0.46	0.42±0.02	26.38±0.35	20.22±0.43	5.02±0.17	31.33±27.18
Dropout	43.71±0.95	58.34±1.00	3.46±0.08	43.26±0.48	29.60±0.80	0.36±0.07	15.69±0.27	17.78±0.38	3.76±0.13	24.00±19.64
Distillation	50.26±0.92	40.17±0.92	65.88±0.56	3.64±0.11	22.28±0.47	0.40±0.07	21.36±0.20	18.06±0.43	5.28±0.07	25.26±21.24
Dropout-Adv	43.21±0.34	47.25±0.98	37.76±0.61	59.32±0.61	49.90±0.37	42.36±1.12	36.82±0.52	37.90±0.84	21.36±0.69	41.76±9.91
Magnet	44.67±0.62	54.72±1.11	44.02±0.31	17.15±0.29	46.60±0.71	60.40±1.20	30.17±0.49	33.47±0.43	11.76±0.25	38.11±15.44
RS-1	77.29±0.58	67.85±0.53	79.77±0.49	9.06±0.22	41.64±0.50	1.19±0.11	54.31±0.57	47.60±0.89	13.96±0.43	43.63±27.97
RS-1-Dropout	50.67±0.44	57.57±0.52	54.81±0.54	7.42±0.37	35.99±0.89	1.46±0.08	33.76±0.38	38.12±0.63	10.26±0.28	32.23±19.97
RS-1-Adv	66.67±0.57	62.85±0.36	64.53±0.52	21.73±0.91	43.96±0.38	9.23±0.39	61.80±0.73	58.55±0.80	38.40±0.86	47.52±19.57
All	56.48±0.74	54.58±0.65	58.45±0.27	10.50±0.16	33.94±0.51	10.79±0.16	30.19±0.24	28.86±0.38	10.02±0.16	32.65±18.91
$L_2 : 2.25 - 2.5$										
Standard	79.11±0.33	63.92±0.94	78.22±0.54	5.10±0.13	37.47±0.94	0.11±0.00	35.33±0.44	28.22±0.47	5.10±0.20	36.95±29.20
Dropout	50.73±0.78	67.29±0.61	6.25±0.23	49.14±0.60	42.66±0.84	0.00±0.00	21.53±0.35	26.97±0.68	5.65±0.23	30.02±22.33
Distillation	58.40±0.66	53.49±0.68	72.94±0.73	4.78±0.10	32.64±0.80	0.00±0.00	30.49±0.50	28.56±0.52	6.82±0.26	32.01±24.15
Dropout-Adv	45.38±0.64	55.61±0.58	37.10±0.58	62.37±0.72	53.10±1.12	45.19±0.68	35.55±0.55	39.02±0.89	16.27±0.53	42.82±12.79
Magnet	50.62±0.43	62.85±0.58	48.72±0.32	21.43±0.42	56.12±0.62	71.37±0.98	33.72±0.33	41.73±1.25	12.02±0.45	44.29±18.14
RS-1	78.37±0.30	73.45±0.65	81.60±0.55	9.45±0.29	48.39±0.75	0.05±0.07	58.84±0.62	54.80±0.81	12.64±0.61	46.40±29.59
RS-1-Dropout	52.26±0.40	60.62±0.71	57.20±0.49	9.78±0.30	41.89±0.56	0.23±0.08	36.38±0.71	45.50±0.78	9.97±0.29	34.87±21.29
RS-1-Adv	72.10±0.45	69.23±0.66	73.20±0.43	28.77±0.37	52.78±0.51	2.06±0.39	66.68±1.04	70.16±0.86	43.36±0.77	53.15±23.09
All	61.17±0.34	63.65±0.54	62.58±0.36	15.32±0.19	44.77±0.65	13.94±0.09	37.62±0.37	39.34±0.58	11.80±0.21	38.91±20.06
$L_2 : 2.5 - 2.75$										
Standard	79.88±0.64	67.38±0.59	81.81±0.45	5.97±0.22	45.13±0.63	0.00±0.00	39.25±0.44	33.73±0.61	6.08±0.19	39.91±29.94
Dropout	49.53±0.89	72.31±0.56	7.14±0.22	52.68±0.56	47.96±0.58	0.10±0.00	25.16±0.38	30.28±0.75	4.84±0.20	32.22±23.66
Distillation	66.82±0.58	62.76±0.46	79.38±0.44	8.17±0.35	44.18±0.57	0.00±0.00	40.56±0.43	38.94±0.71	8.62±0.20	38.83±26.66
Dropout-Adv	44.19±0.60	55.28±0.24	38.23±0.35	66.99±0.95	56.67±0.93	39.81±0.89	34.72±0.55	39.79±0.95	18.59±0.24	43.81±13.42
Magnet	48.42±0.71	60.13±0.56	46.85±0.52	21.31±0.29	55.72±0.44	70.99±0.87	36.16±0.56	44.03±0.78	12.96±0.20	44.06±17.31
RS-1	75.20±0.47	69.54±0.33	78.89±0.35	13.32±0.33	53.34±0.62	0.11±0.00	60.32±0.42	57.60±0.55	14.87±0.42	47.02±27.92
RS-1-Dropout	52.72±0.43	64.07±0.64	57.42±0.67	10.95±0.31	46.80±0.64	0.13±0.00	39.54±0.33	49.82±0.61	10.52±0.38	36.89±22.12
RS-1-Adv	73.92±0.36	70.21±0.48	71.39±0.37	32.02±0.72	52.98±0.53	0.49±0.18	66.84±0.42	69.81±0.58	43.61±0.81	53.47±23.17
All	61.61±0.48	65.56±0.34	63.85±0.31	18.54±0.24	50.09±0.43	13.96±0.11	41.87±0.29	44.28±0.54	13.59±0.18	41.48±20.08
$L_2 : 2.75 - 3$										
Standard	80.66±0.90	71.32±0.45	81.06±0.30	8.57±0.33	49.05±0.23	0.00±0.00	45.83±0.54	41.42±0.62	7.71±0.17	42.85±29.81
Dropout	55.85±0.62	76.08±0.41	10.63±0.32	61.06±0.72	56.14±0.40	0.00±0.00	30.80±0.37	40.78±0.61	7.09±0.17	37.60±25.47
Distillation	69.71±0.45	65.13±0.33	80.32±0.48	9.89±0.20	49.52±0.49	0.00±0.00	45.71±0.17	44.36±0.27	11.74±0.12	41.82±27.00
Dropout-Adv	44.98±0.30	56.20±0.69	40.79±0.45	69.91±0.40	58.80±0.55	29.05±1.07	37.08±0.34	42.75±0.66	16.48±0.39	44.00±15.22
Magnet	51.19±0.70	65.08±0.36	51.43±0.59	27.67±0.39	60.63±0.49	78.24±0.55	39.79±0.48	49.27±0.82	14.88±0.31	48.69±18.15
RS-1	76.38±0.41	75.93±0.35	81.99±0.23	13.41±0.28	56.50±0.45	0.00±0.00	63.22±0.49	61.27±0.59	16.79±0.41	49.50±29.21
RS-1-Dropout	56.66±0.64	68.35±0.55	62.64±0.48	15.40±0.45	51.91±0.38	0.05±0.06	45.23±0.40	55.05±0.94	14.76±0.43	41.12±23.14
RS-1-Adv	70.58±0.35	70.12±0.41	70.51±0.43	35.99±0.95	58.36±0.50	0.34±0.00	69.61±0.42	70.85±0.44	44.53±0.63	54.54±22.72
All	63.58±0.39	68.95±0.15	66.53±0.26	23.05±0.31	55.14±0.30	13.50±0.09	46.88±0.20	50.39±0.42	16.23±0.19	44.92±20.60
$L_2 : 3 - 3.25$										
Standard	84.12±0.53	73.64±0.37	83.74±0.47	10.84±0.21	52.80±0.69	0.09±0.00	51.22±0.76	46.44±0.61	9.94±0.20	45.87±30.48
Dropout	59.16±1.04	79.67±0.31	11.90±0.22	61.54±0.41	57.95±0.51	0.00±0.00	33.53±0.58	43.12±0.47	6.69±0.21	39.29±26.41
Distillation	79.51±0.67	75.82±0.54	87.20±0.28	14.48±0.33	59.77±0.42	0.00±0.00	55.87±0.63	55.42±0.60	14.87±0.57	49.21±29.95
Dropout-Adv	45.28±0.37	60.37±0.72	42.54±0.34	74.24±0.36	60.23±0.32	17.49±0.75	39.70±0.26	45.41±0.82	18.62±0.52	44.76±17.50
Magnet	54.42±0.37	66.97±0.33	56.71±0.50	34.07±0.48	64.50±0.57	79.50±0.51	43.40±0.38	54.87±0.64	17.59±0.21	52.45±17.49
RS-1	76.26±0.44	75.73±0.38	80.65±0.28	17.03±0.41	58.82±0.44	0.10±0.00	65.61±0.56	64.57±0.42	18.36±0.25	50.79±28.67
RS-1-Dropout	60.72±0.68	71.59±0.40	64.81±0.32	21.10±0.81	56.61±0.41	0.00±0.00	49.08±0.39	61.10±0.79	17.47±0.41	44.72±23.83
RS-1-Adv	69.69±0.29	71.49±0.49	70.01±0.28	40.87±0.69	59.04±0.34	0.44±0.05	69.47±0.52	72.33±0.53	48.53±0.77	55.76±22.25
All	65.95±0.37	71.76±0.21	68.02±0.21	28.41±0.31	58.72±0.30	13.08±0.08	50.83±0.33	55.20±0.47	19.00±0.19	47.89±20.84
$L_2 : \geq 3.25$										
Standard	91.23±0.27	86.26±0.21	91.10±0.12	33.24±0.37	70.28±0.49	0.00±0.00	70.78±0.42	66.08±0.53	25.57±0.27	59.39±30.53
Dropout	79.99±0.59	93.75±0.18	41.90±0.27	81.61±0.28	79.70±0.39	0.00±0.00	60.82±0.42	72.37±0.45	24.88±0.37	59.45±29.26
Distillation	92.94±0.21	92.56±0.13	96.48±0.04	55.85±0.33	84.04±0.23	0.00±0.00	82.99±0.26	83.81±0.28	49.83±0.36	70.94±29.42
Dropout-Adv	60.51±0.36	74.84±0.41	57.64±0.45	87.65±0.18	72.75±0.38	3.21±0.24	57.60±0.43	63.53±0.77	39.64±0.71	57.49±22.99
Magnet	68.92±0.35	81.16±0.23	70.91±0.17	61.76±0.26	77.70±0.34	91.11±0.16	62.04±0.30	71.91±0.44	35.51±0.36	69.00±14.71
RS-1	86.84±0.14	87.06±0.13	88.46±0.13	48.72±0.40	74.21±0.46	0.00±0.00	81.73±0.24	80.38±0.32	45.16±0.33	65.84±27.88
RS-1-Dropout	82.47±0.16	90.73±0.14	86.50±0.06	60.83±0.35	81.20±0.32	0.00±0.00	77.28±0.25	86.66±0.26	51.96±0.20	68.63±27.09
RS-1-Adv	76.68±0.25	80.38±0.25	76.81±0.15	63.39±0.44	69.29±0.37	0.06±0.00	78.10±0.31	79.49±0.25	64.58±0.47	65.42±23.88
All	79.22±0.17	85.30±0.14	80.41±0.09	58.67±0.25	76.03±0.32	11.44±0.03	71.77±0.24	75.91±0.33	43.82±0.31	64.73±22.35

Fig. 5: Average passing rate of 5/7 validation (MNIST)

Each column represents a target scheme. This heat map shows which scheme generates better adversarial examples for each target scheme under a fixed L_2 allowance.

	Standard	Dropout	Distillation	Dropout-Adv	RC	Magnet	RS-1	RS-1-Dropout	RS-1-Adv	All
$L_2 : 0 - 0.4$										
Standard	42.35±1.66	29.71±1.80	24.20±0.48	2.69±0.13	7.98±0.31	6.06±0.26	2.81±0.13	2.30±0.25	1.56±0.05	13.30±14.15
Dropout	47.12±0.91	42.72±0.87	31.41±0.38	3.89±0.10	11.49±0.23	7.91±0.10	3.53±0.14	3.56±0.10	1.88±0.06	17.06±17.17
Distillation	29.86±1.24	24.84±1.36	30.07±1.04	2.09±0.14	5.48±0.22	4.71±0.17	1.95±0.11	1.56±0.20	1.38±0.00	11.33±12.14
Dropout-Adv	56.68±0.89	59.33±1.02	54.79±0.34	40.41±1.03	41.18±0.93	49.57±0.90	25.09±1.02	28.77±1.33	14.04±0.59	41.10±14.85
Magnet	47.97±0.67	44.82±0.72	38.03±0.60	14.48±0.40	30.24±0.63	42.74±0.91	12.39±0.85	13.62±0.45	6.57±0.21	27.87±15.28
RS-1	27.74±1.31	24.47±0.90	22.42±0.58	8.60±0.20	16.46±0.94	14.56±0.37	28.06±0.42	16.77±0.78	7.12±0.39	18.47±7.33
RS-1-Dropout	25.45±0.60	27.44±0.75	24.26±0.96	13.24±0.48	20.40±0.27	19.03±0.42	21.88±0.77	26.87±0.80	9.94±0.53	20.95±5.75
RS-1-Adv	47.01±1.06	50.19±2.23	41.98±1.17	41.04±1.29	45.90±0.65	45.34±2.68	45.71±1.28	58.58±2.66	38.06±1.49	45.98±5.86
All	38.50±1.03	32.85±0.95	29.78±0.51	6.51±0.06	12.41±0.16	11.82±0.14	7.48±0.17	7.27±0.28	3.79±0.08	16.71±12.46
$L_2 : 0.4 - 0.8$										
Standard	83.66±0.80	75.23±1.06	68.70±0.89	2.83±0.10	38.22±1.40	4.15±0.19	4.73±0.18	3.60±0.11	1.49±0.00	31.40±33.39
Dropout	79.89±0.95	78.49±0.38	66.78±0.20	3.36±0.12	47.37±0.61	3.83±0.17	3.82±0.12	4.06±0.22	1.53±0.00	32.13±33.36
Distillation	57.21±1.01	53.54±0.60	61.21±1.04	1.91±0.07	18.47±0.56	2.14±0.18	2.28±0.10	1.99±0.09	0.89±0.10	22.18±25.43
Dropout-Adv	45.37±0.67	45.53±0.92	33.84±0.36	25.02±0.68	33.82±0.92	16.43±0.34	12.27±0.20	14.40±0.66	3.81±0.14	25.61±14.10
Magnet	45.50±0.30	45.91±0.47	32.98±0.36	6.15±0.36	36.88±0.56	41.71±0.56	6.92±0.22	6.88±0.33	1.88±0.13	24.98±17.91
RS-1	45.73±0.41	38.74±1.45	38.67±0.37	2.77±0.25	23.36±0.85	5.61±0.40	43.51±0.62	19.77±0.62	1.83±0.16	24.44±16.95
RS-1-Dropout	41.15±0.60	43.07±1.27	34.92±0.70	5.63±0.38	29.99±1.19	7.51±0.19	29.95±0.71	40.62±1.26	4.21±0.12	26.34±15.21
RS-1-Adv	35.07±0.91	36.84±0.46	31.97±0.35	27.89±0.37	31.58±0.46	26.32±0.46	30.72±0.58	42.37±0.37	21.32±1.37	31.56±5.85
All	56.31±0.42	53.82±0.43	48.00±0.40	7.36±0.11	32.33±0.49	11.34±0.14	15.92±0.17	14.52±0.35	3.02±0.09	26.96±19.81
$L_2 : 0.8 - 1.2$										
Standard	97.52±0.33	94.31±0.94	87.20±0.86	5.99±0.38	82.75±1.30	8.52±0.47	13.10±0.41	8.52±0.58	3.00±0.15	44.54±41.32
Dropout	94.99±0.46	94.84±0.32	86.05±0.48	6.08±0.47	88.42±0.58	6.77±0.24	19.15±0.61	17.70±1.04	1.76±0.20	46.19±40.56
Distillation	77.00±1.21	73.05±0.80	84.63±1.06	1.19±0.29	48.92±1.21	3.08±0.55	1.73±0.00	2.92±0.29	0.87±0.00	32.60±35.41
Dropout-Adv	70.27±1.02	73.94±1.61	60.27±0.42	60.58±2.53	63.99±1.26	24.64±0.43	32.75±0.58	37.09±0.90	4.61±0.00	47.57±22.42
Magnet	79.74±0.52	79.47±0.60	60.29±0.49	12.78±0.69	72.09±0.60	76.20±0.61	18.75±0.32	20.96±0.90	2.28±0.10	46.95±30.61
RS-1	68.32±0.71	63.04±0.71	60.68±0.58	5.24±0.36	50.99±0.70	9.56±0.40	77.14±0.64	48.34±0.71	4.09±0.00	43.04±27.23
RS-1-Dropout	67.30±1.01	69.56±0.76	58.90±0.65	9.16±0.47	57.23±0.87	11.30±0.38	60.39±1.72	72.31±1.25	4.10±0.12	45.58±26.92
RS-1-Adv	40.90±0.64	42.21±1.32	32.53±0.88	25.39±0.59	35.54±1.10	25.69±0.62	30.86±0.66	46.53±0.57	17.51±0.69	33.02±8.81
All	73.22±0.56	72.99±0.39	63.82±0.22	18.77±0.57	62.42±0.43	24.30±0.16	34.09±0.43	34.62±0.64	4.96±0.09	43.24±23.94
$L_2 : 1.2 - 1.6$										
Standard	98.73±0.47	97.03±0.37	94.77±0.47	6.50±0.69	95.55±0.66	7.98±0.60	28.74±1.07	18.57±1.80	1.69±0.00	49.95±42.30
Dropout	96.82±0.27	96.82±0.27	94.07±0.56	11.94±0.60	95.90±0.47	9.96±0.89	30.65±1.01	31.50±1.46	1.34±0.27	52.11±40.19
Distillation	78.29±1.89	80.79±0.46	89.21±1.02	3.16±0.00	68.82±1.28	7.76±0.51	4.21±0.00	8.16±0.46	1.05±0.00	37.94±37.36
Dropout-Adv	83.97±0.70	87.12±1.26	74.55±0.73	89.93±0.80	84.73±0.99	27.26±0.76	48.70±0.65	56.40±1.14	5.31±0.47	62.00±28.29
Magnet	95.05±0.22	94.46±0.20	85.94±0.47	24.41±1.20	92.90±0.44	93.52±0.39	35.56±0.86	42.24±1.27	2.60±0.13	62.97±34.47
RS-1	81.59±0.23	77.44±1.22	73.34±0.72	12.79±0.80	70.36±1.43	26.07±0.47	91.46±0.23	72.07±1.05	7.03±0.00	56.91±30.36
RS-1-Dropout	79.87±1.03	84.83±0.69	74.21±0.73	18.13±0.67	78.92±0.81	25.08±0.57	79.33±0.69	88.50±0.67	8.83±0.37	59.75±30.46
RS-1-Adv	63.23±0.85	66.83±1.40	56.89±1.09	62.40±0.70	60.53±1.42	41.20±1.12	64.54±0.62	76.56±0.79	35.56±1.67	58.64±12.08
All	83.50±0.33	84.75±0.43	77.30±0.29	36.54±0.45	80.51±0.50	36.66±0.32	53.56±0.32	56.46±0.93	9.94±0.35	57.69±24.71
$L_2 : 1.6 - 2$										
Standard	100.00±0.00	100.00±0.00	97.86±0.63	24.88±0.88	100.00±0.00	20.36±0.46	45.95±0.63	42.86±2.18	7.02±0.46	59.88±37.03
Dropout	100.00±0.00	100.00±0.00	94.98±0.43	30.92±1.26	99.44±0.43	21.32±1.57	49.33±1.93	53.68±1.86	5.36±0.00	61.67±35.66
Distillation	87.96±3.07	91.67±2.45	93.98±1.79	1.39±1.79	80.56±3.07	3.70±0.00	1.39±1.79	3.70±0.00	0.00±0.00	40.48±43.18
Dropout-Adv	93.07±0.97	95.29±0.55	87.28±0.81	97.84±0.00	94.75±0.59	29.71±0.97	62.88±0.80	74.30±0.57	13.69±0.30	72.09±29.22
Magnet	98.78±0.23	99.07±0.00	95.41±0.43	55.00±1.31	99.07±0.00	98.78±0.23	54.42±0.62	67.73±0.90	4.59±0.54	74.76±30.81
RS-1	89.22±0.80	88.29±1.11	80.46±1.08	19.61±1.96	84.70±0.49	29.89±1.15	97.20±0.45	88.43±0.78	7.11±0.28	64.99±33.33
RS-1-Dropout	86.59±0.81	89.00±0.66	80.21±1.04	32.81±2.21	87.43±0.48	31.58±1.60	86.65±1.01	95.70±0.34	12.24±0.45	66.91±30.01
RS-1-Adv	73.37±1.19	78.03±0.94	69.57±0.68	80.57±0.60	76.72±0.83	48.51±0.80	74.95±0.28	86.55±0.53	61.28±1.44	72.17±10.72
All	89.50±0.56	91.20±0.34	84.63±0.45	54.42±0.90	89.86±0.27	43.07±0.68	68.21±0.24	75.07±0.51	19.51±0.34	68.39±23.48
$L_2 : \geq 2$										
Standard	100.00±0.00	100.00±0.00	100.00±0.00	58.72±1.68	98.68±0.00	47.90±1.46	58.05±3.27	61.33±0.82	21.56±0.52	71.80±27.26
Dropout	100.00±0.00	100.00±0.00	100.00±0.00	72.53±1.95	99.39±0.00	29.32±1.98	54.24±1.13	64.43±0.81	14.43±0.30	70.48±30.91
Distillation	86.31±4.41	89.29±3.95	91.07±5.55	8.33±3.15	86.31±5.02	13.10±3.95	3.57±3.95	4.76±0.00	0.00±0.00	42.53±41.23
Dropout-Adv	95.76±0.42	97.83±0.53	92.09±0.76	99.62±0.11	97.89±0.42	31.81±1.85	62.99±1.09	80.92±0.42	43.48±0.75	78.04±24.35
Magnet	99.76±0.00	99.85±0.12	98.89±0.12	89.99±0.89	98.58±0.00	99.70±0.16	73.47±0.96	81.92±0.27	30.94±0.85	85.90±21.39
RS-1	96.82±0.44	95.42±0.54	92.53±0.58	69.78±1.79	95.23±0.40	28.15±1.71	99.23±0.10	96.42±0.20	46.72±0.87	78.92±24.14
RS-1-Dropout	95.89±0.36	96.71±0.25	91.06±0.28	81.36±1.37	94.67±0.20	38.16±2.10	95.67±0.39	98.85±0.18	53.43±0.92	82.87±20.72
RS-1-Adv	90.77±0.71	92.56±0.55	86.73±0.53	97.76±0.16	87.82±0.46	35.17±1.92	90.93±0.41	97.68±0.12	93.92±0.41	85.93±18.32
All	95.35±0.39	96.13±0.29	92.11±0.29	86.25±0.75	92.32±0.20	43.08±1.49	82.36±0.59	88.89±0.20	56.15±0.42	81.40±17.75

Fig. 6: Average passing rate of 5/7 validation (Fashion-MNIST)

Each column represents a target scheme. This heat map shows which scheme generates better adversarial examples for each target scheme under a fixed L_2 allowance.

	Standard	Dropout	Distillation	Dropout-Adv	RC	Magnet	RS-1	RS-1-Dropout	RS-1-Adv	All
$L_2 : 0 - 0.4$										
Standard	35.00±0.42	33.01±0.18	28.53±2.26	1.29±0.07	19.89±0.18	1.75±0.19	0.67±0.00	1.29±0.14	0.23±0.08	13.52±14.50
Dropout	37.18±0.21	34.99±0.47	31.38±1.25	1.89±0.18	22.85±0.41	1.79±0.17	0.68±0.00	1.11±0.12	0.57±0.08	14.72±15.55
Distillation	47.80±0.62	42.84±0.21	37.79±2.03	1.01±0.12	22.61±0.44	3.91±0.52	0.77±0.09	1.01±0.12	0.66±0.12	17.60±19.13
Dropout-Adv	6.06±0.24	5.46±0.30	3.67±0.51	24.45±0.84	3.37±0.27	3.79±0.28	0.80±0.00	0.87±0.10	0.82±0.16	5.48±6.97
Magnet	35.47±0.85	29.43±1.25	12.87±1.73	4.00±0.38	14.41±1.07	14.90±1.34	0.86±0.33	1.48±0.00	1.35±0.41	12.75±11.95
RS-1	20.97±1.13	21.80±1.05	14.67±0.55	3.51±0.21	11.83±0.54	7.95±0.40	6.20±0.00	6.10±0.27	2.22±0.20	10.58±6.84
RS-1-Dropout	21.13±0.59	21.13±0.63	12.55±1.40	2.82±0.28	11.66±1.08	7.79±0.55	5.49±0.33	6.17±0.28	1.57±0.28	10.04±6.86
RS-1-Adv	16.18±0.85	20.96±1.29	12.75±2.02	21.94±1.38	12.25±0.49	16.54±1.51	9.07±0.81	12.25±1.47	4.04±0.77	14.00±5.46
All	30.25±0.25	28.23±0.29	22.79±1.36	6.34±0.19	16.34±0.22	4.84±0.21	1.82±0.05	2.28±0.13	0.94±0.10	12.65±11.22
$L_2 : 0.4 - 0.8$										
Standard	93.03±0.00	92.54±0.10	85.14±2.49	4.49±0.28	80.70±0.58	1.11±0.17	2.44±0.33	3.55±0.23	0.57±0.08	40.40±42.61
Dropout	92.76±0.08	92.60±0.08	88.31±1.98	7.08±0.43	84.37±0.39	1.71±0.10	3.17±0.16	4.46±0.47	0.69±0.08	41.68±42.88
Distillation	82.94±0.40	80.63±0.25	76.92±1.85	2.55±0.15	58.50±0.67	3.35±0.27	1.54±0.11	2.57±0.36	0.33±0.07	34.37±36.70
Dropout-Adv	21.72±0.46	23.93±0.87	14.16±1.23	89.53±0.21	13.14±0.39	11.39±0.31	1.00±0.15	1.48±0.37	1.21±0.08	19.73±25.96
Magnet	65.10±0.60	62.72±0.44	54.69±1.92	42.11±0.30	55.45±0.51	52.28±0.24	12.36±0.46	14.99±0.60	3.39±0.15	40.34±22.33
RS-1	63.11±0.46	63.00±0.39	59.57±0.61	26.84±0.31	56.17±0.31	33.96±0.48	50.79±0.73	49.18±1.39	7.99±0.36	45.62±17.83
RS-1-Dropout	62.08±0.45	61.94±0.19	59.72±0.53	27.66±0.54	54.87±0.33	32.88±0.49	50.05±0.53	51.61±1.03	8.21±0.44	45.45±17.53
RS-1-Adv	43.00±0.32	42.72±0.64	38.88±0.96	49.29±0.59	36.94±0.45	38.18±0.50	36.31±0.47	35.86±0.60	33.04±0.11	39.36±4.65
All	66.81±0.13	66.35±0.19	61.03±1.41	29.61±0.10	55.74±0.30	19.48±0.18	18.01±0.19	18.77±0.53	5.89±0.11	37.97±22.84
$L_2 : 0.8 - 1.2$										
Standard	100.00±0.00	100.00±0.00	99.64±0.24	12.14±0.67	99.17±0.27	0.58±0.00	10.04±0.46	11.16±0.75	1.74±0.00	48.27±46.15
Dropout	100.00±0.00	100.00±0.00	99.83±0.13	20.26±0.50	99.73±0.00	0.47±0.22	12.20±0.35	13.74±1.08	1.21±0.33	49.72±45.24
Distillation	99.80±0.15	99.40±0.29	99.48±0.15	8.45±0.31	94.33±0.54	2.90±0.19	5.28±0.52	7.86±0.63	0.95±0.00	46.49±46.37
Dropout-Adv	57.04±0.85	58.68±0.53	41.45±2.11	99.84±0.12	43.28±0.67	25.45±0.78	5.37±0.30	7.07±0.39	5.62±0.37	38.20±29.60
Magnet	98.34±0.12	97.43±0.21	96.12±0.38	85.78±0.58	96.68±0.21	96.49±0.00	42.32±0.71	40.57±1.27	12.03±0.60	73.97±31.19
RS-1	96.27±0.21	96.21±0.29	90.01±1.12	58.61±0.58	91.49±0.39	40.73±0.92	80.80±0.66	79.02±1.50	21.17±0.69	72.70±25.27
RS-1-Dropout	96.01±0.36	95.76±0.19	91.09±1.13	58.01±0.88	92.82±0.37	45.67±0.99	83.42±0.82	85.12±0.99	22.96±1.08	74.54±24.68
RS-1-Adv	82.64±0.46	83.13±0.23	79.27±0.47	87.09±0.22	77.20±0.51	72.66±1.00	85.06±0.12	84.71±0.34	79.51±0.67	81.25±4.29
All	90.98±0.16	91.04±0.10	86.65±0.68	55.53±0.25	86.53±0.24	37.07±0.33	41.75±0.27	42.30±0.77	18.37±0.33	61.14±26.36
$L_2 : 1.2 - 1.6$										
Standard	100.00±0.00	100.00±0.00	100.00±0.00	31.84±0.92	100.00±0.00	0.15±0.20	25.82±0.57	27.93±1.48	3.09±0.36	54.32±42.06
Dropout	100.00±0.00	100.00±0.00	100.00±0.00	38.86±1.11	99.62±0.00	0.14±0.18	25.70±0.59	28.90±1.17	5.17±0.25	55.38±41.31
Distillation	100.00±0.00	100.00±0.00	100.00±0.00	18.00±0.79	98.57±0.26	2.24±0.42	12.91±1.32	13.86±1.51	0.61±0.57	49.58±45.08
Dropout-Adv	78.57±0.62	77.02±0.72	70.11±1.91	100.00±0.00	68.84±0.75	36.09±0.66	15.05±0.63	18.84±1.01	12.28±0.54	52.98±30.81
Magnet	100.00±0.00	100.00±0.00	100.00±0.00	98.77±0.25	100.00±0.00	99.17±0.15	71.68±0.88	72.78±1.52	26.50±0.72	85.43±23.67
RS-1	99.78±0.17	98.97±0.38	98.35±0.17	78.79±0.78	98.12±0.30	48.30±1.33	97.32±0.47	95.71±0.99	39.37±1.27	83.86±22.34
RS-1-Dropout	98.99±0.33	98.72±0.17	97.89±0.00	82.88±0.55	97.36±0.35	49.69±1.31	96.92±0.52	98.02±0.17	44.01±1.44	84.94±20.95
RS-1-Adv	96.41±0.28	95.23±0.53	93.09±0.60	98.95±0.34	93.27±0.26	82.68±0.44	97.45±0.48	97.27±0.57	91.68±0.84	94.01±4.62
All	96.52±0.13	96.02±0.17	94.63±0.33	72.14±0.41	94.21±0.18	43.36±0.48	58.16±0.27	59.46±0.95	29.47±0.54	71.55±23.95
$L_2 : 1.6 - 2$										
Standard	100.00±0.00	100.00±0.00	100.00±0.00	50.83±1.27	99.34±0.00	0.00±0.00	39.65±1.07	39.98±1.10	7.62±0.66	59.71±38.86
Dropout	100.00±0.00	100.00±0.00	100.00±0.00	62.15±1.34	100.00±0.00	0.00±0.00	48.87±1.09	47.66±2.84	7.03±0.73	62.86±38.04
Distillation	100.00±0.00	100.00±0.00	100.00±0.00	38.39±1.19	100.00±0.00	2.98±0.34	28.97±1.32	33.23±1.15	6.35±0.00	56.66±40.25
Dropout-Adv	85.88±0.77	86.17±1.05	77.32±0.97	100.00±0.00	77.32±1.25	40.03±1.34	22.68±0.48	22.12±1.22	18.75±0.84	58.92±30.70
Magnet	97.54±0.26	97.24±0.00	96.46±0.00	96.21±0.19	96.85±0.00	95.32±0.24	82.14±0.48	77.17±2.25	37.65±1.11	86.29±18.60
RS-1	99.69±0.24	99.50±0.00	99.06±0.53	90.81±0.66	98.69±0.24	42.50±1.62	100.00±0.00	98.69±0.24	58.62±1.32	87.51±20.30
RS-1-Dropout	99.23±0.23	99.06±0.00	98.47±0.20	87.74±0.62	98.94±0.20	44.58±1.90	100.00±0.00	100.00±0.00	62.50±1.08	87.83±19.17
RS-1-Adv	98.32±0.00	99.05±0.28	98.21±0.35	99.58±0.00	98.90±0.20	69.22±1.20	99.58±0.00	99.05±0.28	99.16±0.00	95.68±9.37
All	97.50±0.12	97.55±0.15	96.09±0.21	82.61±0.39	96.22±0.18	44.00±0.50	70.84±0.27	69.95±0.91	42.87±0.50	77.51±20.94
$L_2 : \geq 2$										
Standard	100.00±0.00	100.00±0.00	100.00±0.00	76.12±0.99	100.00±0.00	0.23±0.20	69.56±1.00	64.62±2.69	34.10±0.22	71.63±33.01
Dropout	100.00±0.00	100.00±0.00	100.00±0.00	78.10±1.29	100.00±0.00	0.30±0.17	63.85±0.96	61.35±2.25	22.20±0.82	69.53±34.85
Distillation	100.00±0.00	100.00±0.00	100.00±0.00	63.51±1.78	99.70±0.00	13.29±1.00	60.93±0.72	58.08±1.67	23.50±0.70	68.78±32.01
Dropout-Adv	95.66±0.52	96.27±0.45	91.49±1.14	100.00±0.00	92.49±0.62	41.06±1.51	44.57±0.78	42.49±0.81	40.67±0.68	71.63±26.46
Magnet	100.00±0.00	100.00±0.00	100.00±0.00	99.84±0.00	100.00±0.00	96.13±0.38	96.86±0.16	95.62±0.83	70.99±1.03	95.49±8.85
RS-1	99.83±0.00	100.00±0.00	99.73±0.08	92.16±0.65	99.23±0.08	19.43±0.99	100.00±0.00	99.83±0.00	91.49±0.63	89.08±24.84
RS-1-Dropout	99.83±0.00	99.78±0.14	99.83±0.00	94.93±0.55	99.43±0.14	22.37±1.13	100.00±0.00	100.00±0.00	93.39±0.26	89.95±24.01
RS-1-Adv	92.43±0.63	91.28±0.55	90.19±1.03	95.14±0.34	88.80±0.42	14.35±0.36	100.00±0.00	99.92±0.06	100.00±0.00	85.79±25.60
All	97.98±0.14	97.79±0.12	97.16±0.18	90.26±0.45	96.77±0.12	29.40±0.34	86.91±0.23	85.68±0.70	71.07±0.36	83.67±20.87

Fig. 7: Average passing rate of 5/7 validation (CIFAR-10)

Each column represents a target scheme. This heat map shows which scheme generates better adversarial examples for each target scheme under a fixed L_2 allowance.